National Library of Canada
Bibliothèque nationale du Canada

Acquisitions and Bibliographic Services Branch
Direction des acquisitions et des services bibliographiques

395 Wellington Street
Ottawa, Ontario
K1A 0N4

395, rue Wellington
Ottawa (Ontario)
K1A 0N4

Your file Votre référence

Our file Notre référence

NOTICE

The quality of this microform is heavily dependent upon the quality of the original thesis submitted for microfilming. Every effort has been made to ensure the highest quality of reproduction possible.

If pages are missing, contact the university which granted the degree.

Some pages may have indistinct print especially if the original pages were typed with a poor typewriter ribbon or if the university sent us an inferior photocopy.

Reproduction in full or in part of this microform is governed by the Canadian Copyright Act, R.S.C. 1970, c. C-30, and subsequent amendments.

AVIS

La qualité de cette microforme dépend grandement de la qualité de la thèse soumise au microfilmage. Nous avons tout fait pour assurer une qualité supérieure de reproduction.

S'il manque des pages, veuillez communiquer avec l'université qui a conféré le grade.

La qualité d'impression de certaines pages peut laisser à désirer, surtout si les pages originales ont été dactylographiées à l'aide d'un ruban usé ou si l'université nous a fait parvenir une photocopie de qualité inférieure.

La reproduction, même partielle, de cette microforme est soumise à la Loi canadienne sur le droit d'auteur, SRC 1970, c. C-30, et ses amendements subséquents.

Canada

Single Crystal Growth and Analysis of Germanium

RICARDO JARAMILLO

A Thesis

in

The Department

of

Electrical and Computer Engineering

Presented in Partial Fulfillment of the Requirements
for the degree of Master's of Engineering at
Concordia University
Montreal, Canada

February 1989

© RICARDO JARAMILLO, 1989

National Library of Canada

Bibliothèque nationale du Canada

Acquisitions and Bibliographic Services Branch

Direction des acquisitions et des services bibliographiques

395 Wellington Street
Ottawa, Ontario
K1A 0N4

395, rue Wellington
Ottawa (Ontario)
K1A 0N4

Your file Votre référence

Our file Notre référence

The author has granted an irrevocable non-exclusive licence allowing the National Library of Canada to reproduce, loan, distribute or sell copies of his/her thesis by any means and in any form or format, making this thesis available to interested persons.

L'auteur a accordé une licence irrévocable et non exclusive permettant à la Bibliothèque nationale du Canada de reproduire, prêter, distribuer ou vendre des copies de sa thèse de quelque manière et sous quelque forme que ce soit pour mettre des exemplaires de cette thèse à la disposition des personnes intéressées.

The author retains ownership of the copyright in his/her thesis. Neither the thesis nor substantial extracts from it may be printed or otherwise reproduced without his/her permission.

L'auteur conserve la propriété du droit d'auteur qui protège sa thèse. Ni la thèse ni des extraits substantiels de celle-ci ne doivent être imprimés ou autrement reproduits sans son autorisation.

ISBN 0-315-80985-X

Canada

ABSTRACT

Single Crystal Growth and Analysis
of Germanium

Several large diameter (>5.0 cm.) germanium single crystals were grown in a vertical Czochralski crystal grower. Some of these crystals were intentionally doped with antimony to create n-type, approximately .5 Ω-cm material to act as substrates for later date GaAs heteroepitaxial deposition. The doping was accomplished with the aid of an antimony saturated doping alloy added to the charge prior to melting. The dopant concentration profile throughout the crystal follows the segregation relationship known for "normal freezing" situations.

Experimental techniques such as bulk Hall-Effect analysis, dislocation density determination, and X-ray diffraction were performed to ascertain the qualities of the crystal and assess its suitability as a substrate.

ACKNOWLEDGEMENT

I would like to thank my supervisor, Dr. B. A. Lombos for his help and suggestions in the experimental as well as theoretical work during all phases of the experiment. Equally important throughout this experiment was Dr. Lombos' enthusiasm for the subject and the moral support he provided.

TABLE OF CONTENTS

			Page
		LIST OF ILLUSTRATIONS AND TABLES	vi
CHAPTER 1		INTRODUCTION	1
CHAPTER 2		REVIEW OF CRYSTAL GROWTH CHARACTERISTICS	
	2.1	Impurity Distribution of a Vertical-Pull Crystal	10
	2.2	Crystal Growth Criteria	12
	2.3	Fundamental Aspects of Czochralski Growth	15
CHAPTER 3		EXPERIMENTAL TECHNIQUE OF CRYSTAL GROWTH	
	3.1	Preparations (cleaning)	19
	3.1.1	Growth Chamber Wall / Seed Shaft	20
	3.1.2	Crucible Cleaning	20
	3.1.3	Polycrystalline Ge / seed cleaning	21
	3.2	Growth of Ge Single Crystal	22
	3.3	Creation of Doping Alloy	36
CHAPTER 4		EXPERIMENTAL RESULTS	
	4.1	Preparations Prior to Analysis	40
	4.2	Hall-Effect Measurements	45
	4.2.1	Hall-Effect Measurement Precautions	49
	4.2.2	Resistivity Determination	50
	4.2.3	Hall Coefficient Determination	51
	4.2.4	Sample Calculation	52
	4.2.5	Comments of Results	55
	4.3	Determination of Segregation Coefficient	57
	4.4	Determination of Dislocation Density	60
	4.4.1	Procedure for Developing Etch Pits on <100> Ge	62
	4.5	X-Ray Diffraction	65
CHAPTER 5		SUMMARY AND CONCLUSION	69
		REFERENCES	71
		APPENDIX A	74
		APPENDIX B	75

LIST OF ILLUSTRATIONS AND TABLES

Figure — Page

1.1 Cation/anion planes and antiphase regions of GaAs-on-Si.......... 5

2.1 Basic components of a crystal grower and seed holder.......... 13

2.2 Isothermal surfaces and their effects.......... 17

3.1 Graph illustrating concentration vs resistivity.......... 35

4.1 Seed removed from grown crystal.......... 41

4.2 Hall sample indicating current and voltage terminals.......... 43

4.3 Hall sample with external fields applied.......... 45

4.4 Solute concentration at the solid-liquid interface.......... 57

4.5 Plot of log(C/C_o) vs log(1-X) to determine K_{eff}.......... 59

4.6 SEM micrograph of dislocation pits.......... 64

4.7 Geometrical criteria for X-ray diffraction.......... 65

4.8 X-ray diffraction spectrum of <100> crystal.......... 68

LIST OF TABLES

Number — Page

1.1 Several physical constants for these semiconductors.......... 7

3.1 Characteristics and comments of the crystals grown.......... 30

4.1 Characteristics of the crystals grown.......... 54

4.2 X-ray diffraction angles for crystal plane.......... 67

CHAPTER I

INTRODUCTION

Throughout the past decade, scientific interest in the development of III-V compounds for semiconductor purposes has increased. The most widely studied of the many III-V compounds are GaAs and InP.[1] Microwave devices, such as high frequency oscillators and electrooptic devices, such as LEDs (Light Emitting Diodes) fabricated from GaAs, have in the past been used, and are presently being employed for commercial to military applications. Solar cells and integrated circuits manufactured from GaAs are being investigated seriously.[2]

GaAs photovoltaic cells have a distinct advantage over the common silicon cell due to their higher conversion efficiency, radiation hardness in space environments and greater survivability at elevated temperatures.[3] Integrated circuits, fabricated from GaAs, would have the capacity for high switching speeds due to its (the GaAs's) high electron mobility. Equally, GaAs is capable of processing optical pulses owing to its direct bandgap structure since the electron phonon interaction is minimized. The potential applications for these devices range from high efficiency (>20% Air Mass 0, AM0) solar cells,[4] to high power low noise MESFETs for microwave amplifiers,[5] to high speed logic devices required in next generation super computers.

Conventional manufacturing processes of III-V devices require the

deposition of the active single crystal semiconductor material a few microns thick onto the surface of a single crystal semiconductor wafer. This process is known as epitaxial technology. Various techniques to accomplish epitaxial growth, such as Liquid Phase Epitaxy (LPE), Chemical Vapour Deposition (CVD) and Molecular Beam Epitaxy (MBE) exist. There are advantages and disadvantages associated with each technique. The wafer, generally several hundred microns thick acts as a supporting and heat dissipating substrate. Any possible future development of III-V devices may be impeded by the cost and availability of wafers composed of III-V compounds. To circumvent this potential problem, interest in the development of techniques and materials for the deposition of III-V compounds on inexpensive and easily manageable substrates is intense.

Motivation for the creation of heteroepitaxial III-V compounds on group IV semiconductors, such as Si and Ge, are quite substantial. Silicon-based ICs have demonstrated themselves as the workhorse of the present-day semiconductor industry and hence is the natural choice for substrate material.

The driving forces for GaAs-on-Si technology depends on the desired application, eg., if GaAs-on-Si heterostructures are to be used merely to replace GaAs substrates, then the wafer size, cost, strength, thermal conductivity, and low density of Si substrates become the determining factors.[6]

Where large die sizes are of paramount importance such as for Monolithic Microwave Integrated Circuits (MMICs) and Large Scale Integration (LSI) memory circuits, manufacturing technology is hampered by the low thermal conductivity of GaAs.[7] While GaAs substrates are becoming available in 4" sizes, in laboratories, Si is now available commercially in 8" diameter wafers. This not only increases device heat dissipation but the chip yields during batch processing.[8]

In applications where materials, rather than processing costs predominate, the use of less brittle Si substrates will increase the yield and thus lower the cost of GaAs parts appreciably. They not only reduce wafer breakage, but also eliminate much of the need for custom manufacturing equipment. GaAs wafers need to be much thicker than Si and require specially designed manufacturing equipment, such as cassette-to-cassette loaders, particularly for high density GaAs manufacturing. Use of GaAs on Si can allow the GaAs device manufacturers to use existing Si processing equipment.[9]

GaAs solar cells, can also, benefit from the lower cost of Si substrates. The lower density of Si as compared to GaAs is very advantageous for GaAs-on-Si solar cells intended for space applications, where each pound eliminated can save thousands of dollars. Radiation hardness can also be enhanced by the use of GaAs-on-Si, since GaAs cells appear to have a significantly better radiation resistance than Si

cells.[10]

Notwithstanding all the benefits listed above, there do exist serious problems and elaborate solutions have been found in merging these two semiconductors to form the basis of a viable new technology.

The growth of <100>-oriented GaAs epitaxy entails the formation of alternating layers of Ga and As atomic planes. These layers of atoms are termed as the anion and cation planes respectively. Fig. 1.1 illustrates this layered structure. If the Si surface were atomically flat and the growth occurred by uniform two dimensional nucleation, the first sublattice could be deposited followed by the more conventional epitaxial MBE growth.[11] Experiments, however, have shown that the surface of Si is not atomically flat and initial growth of GaAs on Si occurs by the merging of individual nucleation centers.[12] Owing to the stepped nature of the Si surface, the sticking probabilities of III-V elements and the exchange between the compounds and elemental Si, the surface growth during the first few atomic layers of nucleation centers are all such that they have the same orientation when coalesced. This makes it possible to create alternating cation and anion planes over the entire wafer surface in the <100> direction.[13]

Single phase growth can be assured by tilting the substrate 4° off the <100> direction towards the <110> direction and effecting a two temperature growth. Fig. 1.1 illustrates a crystalline model of GaAs-on-

Si.[14]

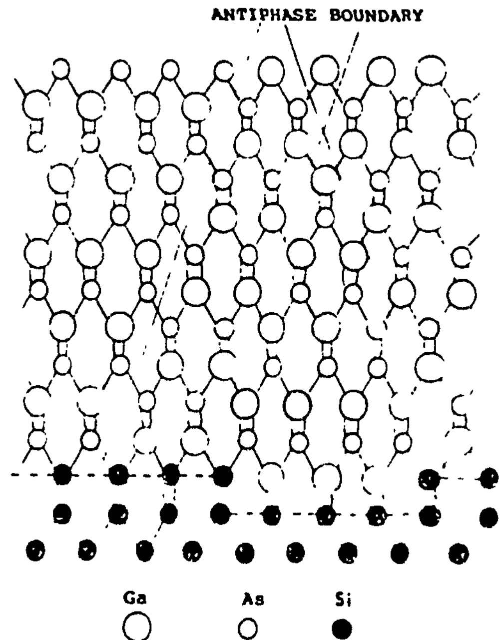

Fig 1.1 Cation/anion planes and antiphase regions of GaAs-on-Si.[15]

Orientations tilted a few degrees off the <100> direction also significantly reduced another crystalline imperfection; threading dislocations caused by the 4.1 percent lattice mismatch.[16] In the early stages of growth, the lattice mismatch is accommodated by compressive strain. After several tens of monolayers are deposited, the strain energy is exceeded resulting in the formation of dislocations. Tilting causes the greatest majority of dislocations to propagate along the interface. Most dislocation threading into the GaAs epilayer are thereby diminished by each other and few reach the surface where they can lead to device degradation.[17]

The progress of GaAs-on-Si technology has been brought on by the advent of improved MBE equipment. An MBE machine functions by evaporating semiconductor material in an ultra-high vacuum system. This setup is capable of synthesizing new layered semiconductor devices exhibiting innovative electronic and photonic properties.

Developments during the last ten years in vacuum technology have improved epitaxial technology to the extent that practically no contamination of the epilayer is present. This has allowed for the controlled deposition of materials on an atomic scale and the construction of devices such as high frequency devices and HEMTs (High Electron Mobility Transistors) whose conduction is best described as a two dimensional electron gas (2DEG).[18]

From the description given above concerning the elaborate and expensive techniques required to realize GaAs-on-Si heteroepitaxial growth, it may be advisable to look for alternative solutions. As can be seen from Table 1.1, the lattice spacing difference between GaAs and Ge is very small, less than the difference between GaAs and Si. It is also seen that their linear coefficient of expansion is very close, hence, it may be hypothesized that GaAs-on-Ge is a very likely candidate for heterostructural devices. It is for these reasons that the epigro-

wth of GaAs-on-Ge should be explored. With the advent of Si based semiconductor devices about 20 years ago, the popularity of Ge has declined, mainly since Ge is now considered a material from an "old technology". Several factors contributed to the idea of growing large diameter, single crystal Ge. Since single crystal Ge is no longer available, it was economically feasible to purchase zone refined polycrystalline (purified to semiconductor grade standards) Ge to grow into single crystals. Furthermore, the Czochralski growth technique is capable of growing crystals with a predetermined doping profile. Lastly the growth of Ge crystals has provided a unique experience of preparing, growing and characterizing a crystal for the use as substrate material required by today's semiconductor industry.

	LATTICE CONSTANT Å	LINEAR COEFFICIENT OF EXPANSION $\delta L / L\delta T$ (°C^{-1})	THERMAL CONDUCTIVITY W/cm-°C
Si	5.43095	2.6×10^{-6}	1.5
Ge	5.64613	5.8×10^{-6}	.6
GaAs	5.6533	6.9×10^{-6}	.46

Table 1.1 Several physical constants for these semiconductors.[19]

CHAPTER II

REVIEW OF CRYSTAL GROWTH CHARACTERISTICS

The electrical behavior of single crystals is highly sensitive to the quality of the crystal perfection and chemical purity. The semiconductor engineer is expected to be knowledgeable in all areas of crystal growth and material characterization. The finished semiconductor crystal may be used either for the fabrication of discrete devices or monolithic integrated circuits. Utilizing any of the well known photolithographic techniques a semiconductor wafer may be used as a substrate in an epitaxial deposition or as a bulk device. However different these semiconductor end products may appear, crystal imperfections of any type can be detrimental to the overall electrical quality of the device.[20]

The techniques for obtaining high purity single crystals with high physical crystal perfection, have received a large amount of attention during the growth of the semiconductor industry. Since virtually every semiconductor device produced uses a single crystal, it is obvious that it is necessary to have rigorous analytical control and examination of both the crystal growth process and the finished crystal itself. Although there are many methods of growing crystals, they all fundamentally involve controlled crystallization of the semiconductor in a very pure form and in a crystallographically perfect arrangement. This crystallization can take place from the melt or from the vapour. Upon examination of the various methods, it is generally found that each

semiconductor (eg., Ge, GaAs, or SiC) is grown by a slightly different method to optimize crystalline perfection and ease of growth.[21]

Silicon and germanium are, by far, the most important and commonly used semiconductors. Their present day development, however, have reached their limits, and only recently have the III-V compounds begun to encroach on the domination of Si and Ge in new high frequency and electrooptic applications.

2.1 IMPURITY DISTRIBUTION OF A VERTICAL-PULLED CRYSTAL

The vertically-pulled crystal growth technique is often referred to as the Czochralski method even though Czochralski originally developed the method to study the speed of crystallization of various metals.[22] Teal and Little modified this technique and applied it to the growth of silicon and germanium single crystals.[23] In general, the vertical pull technique starts by preparing a melt of the semiconductor in a quartz or graphite crucible. A small crystallographic oriented single crystal seed of this semiconductor is introduced onto the surface of the melt and then the seed crystal is rotated while slowly being withdrawn from the melt. By the judicious choice of heat input and pulling rate, the desired crystal shape and size can be grown.

The growth of single crystals by vertically pulling the crystal from the melt has several advantages over other techniques with regard to impurity distribution in the crystal. The continuous stirring by the rotating crystal increases the temperature homogenity throughout the melt as well as providing a uniform impurity distribution. Simultaneously, the large temperature differential at the solid-liquid interface minimizes the movement or diffusion of impurities from the melt into the single crystal.

The vertical puller does not lend itself to the growth of long, uniformly doped single crystals because the dopant or impurity con-

centration in the melt is constantly changing due to the distribution of impurities between the solid and liquid phases. This is characterized by the relationship $K = C_s / C_l$, where C_s is the concentration of impurity in the solid, and C_l is the concentration of impurity in the liquid. As a result, the crystal will show an impurity-concentration distribution that will be graded from the top of the crystal to the bottom. The concentration of the impurity over the length of the pulled crystal is described by the following equation:[24]

$$C_x = KC_o(1-X)^{(K-1)} \qquad [2.1]$$

Where C_o = initial concentration in melt.

C_x = concentration at any point X along the length of the solid crystal.

X = the fraction of the original volume which has solidified ($0 < X < 1$).

K = effective distribution coefficient.

The effective distribution coefficient is slightly different for each apparatus and for each set of pull conditions; and to overcome the difficultly of producing large, uniformly doped single crystals, other horizontal zone refining techniques were developed.[25]

2.2 CRYSTAL GROWTH CRITERIA

Monocomponent growth, of undoped as well doped crystals by establishing a solid-liquid equilibrium is the preferred method of growing semiconductor or metal crystals. Essentially, this technique is used to grow single crystals by pulling it from the melt. In comparison to other techniques, it is an uncomplicated, easily controllable process. The process of pulling cannot be applied to every material. Among the reasons are the following:[26]

1) The material decomposes before it melts thereby requiring a liquid encapsulent be used.

2) Sublimation of the material occurs or has a high vapour pressure at its melting point. This can be seen in several compound semiconductors, requiring expensive fabrication technology.

3) The melting point is so high that it makes growth experimentally impractical.

The present day growth of bulk elemental semiconductor single crystals such as germanium and silicon, evolved from the pioneering efforts of G. Teal and J. Little in 1960. Fig 2.1 illustrates the basic components of a vertical Czochralski crystal grower. The semiconductor material is placed into a suitable crucible, A, which is, in turn, heated by an energy source, B. Both resistance heating and induction

heating have been successfully used. To promote nucleation in a particular crystal orientation a seed, C, is held in a vertically movable shaft, D, and simultaneously rotated if deemed necessary. Also illustrated is the construction of the seed holder.

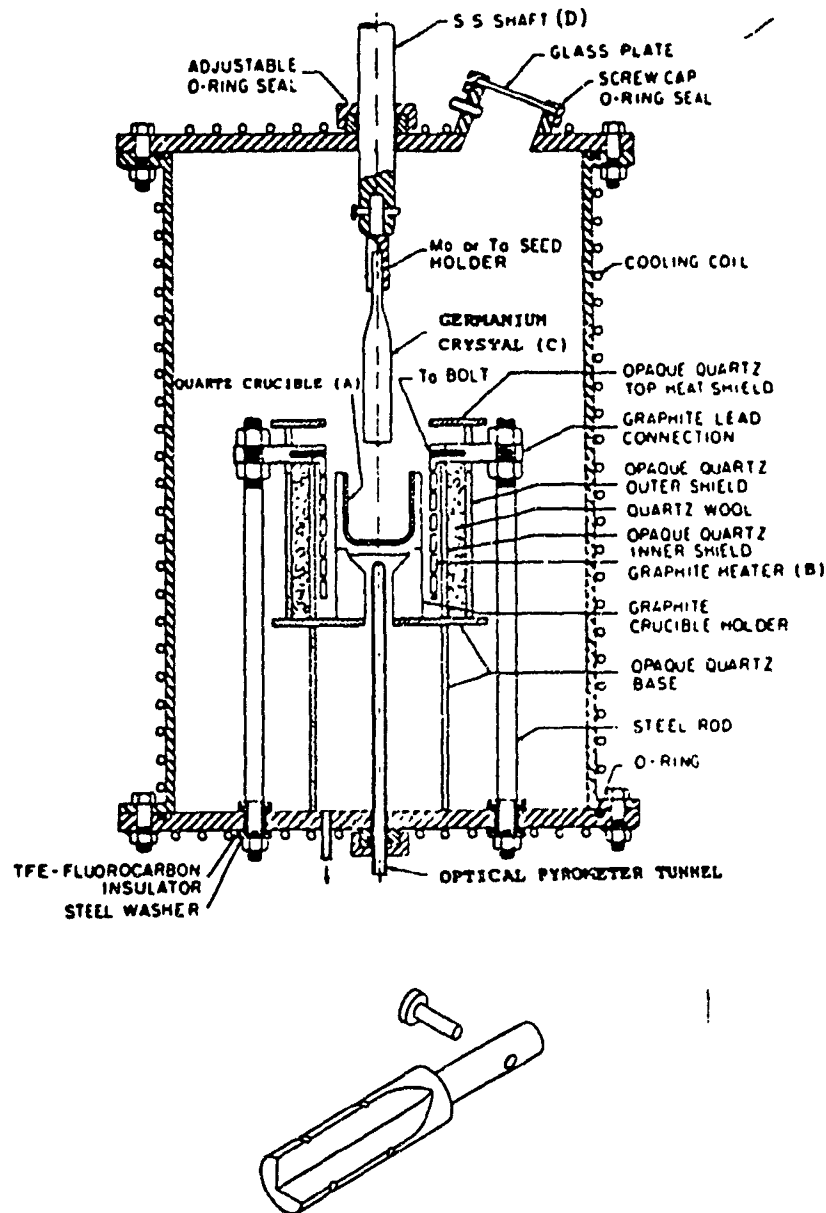

Fig. 2.1 Basic components of a crystal grower and seed holder.

The prime importance of this technique results from the fact that the grown crystal is free of the physical constraints imposed by the crucible. The necessity of having the melt contained within a crucible that might act as a source of contamination, is one of the main disadvantages of this technique. Modifications of this technique, which are crucibleless, have been developed.[27] The prime criteria required for successful pulling of a crystal are the following:

(1) The crystal and crystal plus dopant should form a solution when melted.

(2) The crystal should not react with the crucible or the atmosphere during growth. Inside the growth chamber, inert, oxidizing or reducing atmospheres can be provided to eliminate the formation of undesired compounds.

(3) The melting temperature should be attainable with heaters available and should be below the melting temperature of the crucible.

(4) Process control parameters, such as pulling rates and thermal gradients in the vicinity of the solid-liquid interface, should easily be varied.

2.3 FUNDAMENTAL ASPECTS OF CZOCHRALSKI GROWTH

The principal advantage of pulling crystals from the melt is that growth can easily be achieved on the seed under conditions which are easily controllable. These growth conditions are possible since the seed-melt interface is visible throughout the entire growth procedure.

To commence the growth of a crystal, the melt is held at a temperature slightly above the melting point of the material. The seed is then touched to the surface of the melt in the center of the crucible. Raising the temperature slightly at this point melts a small portion of the seed. This ensures that the melt wets the seed. This may be verified by the appearance of the meniscus formed between the seed and the melt. The temperature is then lowered until the melt begins to freeze onto the seed. At this point, the mechanism, which slowly raises the seed away from the melt, is commenced. As the seed is lifted, the grown portion of the crystal is cooled by conduction along the cold seed and seed holder, as well as conduction and radiation to its immediate surroundings. The operator should have the correct melt temperature at this important phase. If the temperature is too high, the portion of the seed will melt and add to the molten mass. If the temperature is too cool, the solid-liquid interface will suddenly grow outward rapidly, making controlled freezing impossible. Assuming all is fine, growth is continued to any desired point where it can then be stopped by rapidly pulling the growing crystal away from the melt. A skilled operator can

often pull the entire melt from the crucible into a single crystal. Should spurious nucleation occur during the growth, the operator can reverse the growth sending back the portion of the crystal into the melt and raising the temperature a few degrees. Once equilibrium has been achieved, growth of the crystal may resume.

The pulling technique has a further advantage in that the growing crystal and the liquid-solid interface do not contact the crucible surface. The risk of contamination of the grown crystal is greatly reduced. As well, it prevents the creation of mechanical deformation of the crystal which might easily be produced as the crystal cools due to the differences between the thermal contractions of the crystal and the crucible. The perfection of the crystal is impaired by thermal stresses arising from the differential contraction as the crystal is cooled. The separation of the liquid-solid interface from the crucible surface avoids the formation of spurious nucleation. This could result from any chemical reaction between the melt and the fused quartz crucible.

Under normal growing conditions, the temperature of the crucible wall is usually kept above the melting point of the substance in order to prevent spurious nucleation. Under certain conditions, this region may cool below the equilibrium melting point since very pure melts can often be appreciably supercooled without nucleation. In general, however, this condition is rare and with a hot crucible wall, the thermal gradients are such that heat flows from the crucible into the crystal-melt interface, and from there into the grown portion of the

crystal.

From this description it can be presumed that a thermal gradient must exist along the growth axis, and is responsible as the main path of heat removal at the solid-liquid interface. Too large a gradient of an improper shape can have a disastrous effect on the perfection of the crystal. Large temperature differences over small distances of growth length can produce large stresses because of differential thermal contraction. If these stresses exceed the elastic limit of the crystal, it will plastically deform and large concentrations of dislocations and other imperfections will be produced. Assuming that the solid-liquid interface is an isotherm, Fig 2.2 illustrates how the isothermal surfaces within the crystal will look for an interface that appears concave, planar, and convex.[28] The curved interfaces have a transverse and longitudinal gradient components. In the planar case, only longitudinal gradients exist.

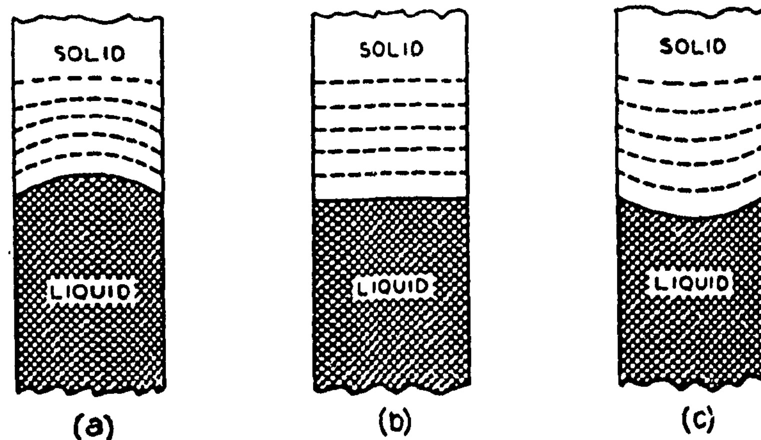

Fig 2.2. Isothermal surfaces and their effects

The rate at which mass of crystal is grown is determined by the differences between these two opposing thermal fluxes. If there is a net accumulation of heat at the solid-liquid interface, the crystal will melt. If there is a net loss of heat at this interface, the crystal will grow at the carefully controlled rate determined by the important process parameters responsible for the dissipation of the heat of fusion. Generally, the thermal conductivities and heat capacities of the liquid and solid semiconductor are not known sufficiently accurately to permit a detailed statement of the conditions necessary to achieve a particular crystal growing result. Furthermore, the conditions change continuously during the growth of the crystal. As the melt is depleted and the crystal grows larger, both the thermal input into the melt and the paths for heat loss change significantly. Thus, the first growth of a crystal is usually carefully monitored. Once the necessary conditions for the desired results are determined, the crystal pulling machine can be programmed to reproduce the necessary conditions.

The shape of the pulled crystal can be determined by controlling the variables during crystal growth. Since the mass of the crystal grown per unit time depends upon the thermal gradients in the melt and the crystal, and the length of the crystal depends on the rate of pull, the diameter of the crystal can be determined by controlling the thermal gradients and/or the rate of pull.

CHAPTER III

EXPERIMENTAL TECHNIQUE OF CRYSTAL GROWING

To commence the growth of Ge crystals, the starting material must be of the highest purity. All of the crystals grown in the Microelectronics laboratory, started with zone refined polycrystalline bars. Since the raw Ge at this point is intrinsic, it is assumed to have an impurity concentration less than 10^{13} at/cm^3. The total quantity of polycrystalline Ge was 2.0 kilograms. This quantity provided four (4) crystals of approximately 500 grams.

3.1 PREPARATIONS (cleaning)

Prior to any crystal growth, cleaning preparations to the crystal grower, as well as the Ge must be performed. This is to ensure that no contamination enters into the melt, thereby altering physical and / or electrical characteristics of the end-product. The areas to consider are the following;

1) Crystal grower chamber wall and seed shaft.
2) Fused silica crucible
3) Polycrystalline charge and seed.

3.1.1 GROWTH CHAMBER WALL / SEED SHAFT

The interior surface of the crystal grower is constructed of polished, stainless steel. Trichloroethane, acetone and methanol are individually soaked into lint free tissue paper and used to wipe down the interior of the growth chamber. During this operation, plastic gloves are worn to ensure that no contamination from the hands are deposited on the interior. The function of these degreasers is to dissolve and remove any organic substances which are accidentally placed there during everyday handling. The seed shaft is also constructed of stainless steel, however, it is terminated with a molybdenum dowel to which the seed is attached. Molybdenum has a very high melting point as well as a low vapour pressure and hence can be used near to the melt surface. For this reason, it is important to have the seed shaft clean. The seed shaft is cleaned in the same manner as the growth chamber. Following the cleaning of the growth chamber and seed shaft, the grower is reassembled and pumped down to approximately 1.3 Pa. and left sealed until the raw Ge and seed are cleaned.

3.1.2 CRUCIBLE CLEANING

Boiling trichloroethane, acetone and methanol are used individually two to three times to clean the fused silica crucible. Following the organic degreasing, the interior of the crucible is etched with a

buffered solution of hydrofluoric acid (HNO_3 / HF 4:1 by volume) for five to ten minutes. The purpose of the etchant is to remove any inorganic substances incorporated or diffused into the fused silica. Following the etching procedure, the crucible is rinsed with deionized water several times. The crucible is then left to outgas in an oven of approximately 100°C to remove any moisture from its surface.

3.1.3 POLYCRYSTALLINE Ge/SEED CLEANING

The cleaning process for the polycrystalline Ge and seed involves boiling in the same degreasers mentioned earlier. In addition to the organic removal a powerful oxide remover is prepared prior to the material entering the growth chamber. The polishing solution consists of;

5 parts by volume	Acetic Acid CH_3COOH
10 parts by volume	Nitric Acid HNO_3
5 parts by volume	Hydrofluoric Acid HF
2 - 3 mls	Bromine Br_2

Owing to the nature of these chemicals, acid resistant gloves and

goggles are worn. The preparation of this solution is preformed in a Teflon beaker due to the etching characteristics of the hydrofluoric acid. The polycrystalline Ge is slowly immersed into the polishing solution for 45 - 60 seconds. The ensuing chemical reaction is a vigorous bubbling action. After the reaction is completed the polycrystalline Ge has a brilliant metallic appearance. Following the acid solution it is necessary to rinse the Ge with deionized water several times. The last rinsing of the Ge is accomplished in an ultrasonic bath for 15 minutes. Once the Ge is cleaned, it is left to outgas in the oven for 30 minutes. This operation is repeated for the seed.

3.2 GROWTH OF Ge SINGLE CRYSTAL

Provided the growth chamber and polycrystalline Ge are satisfactorily cleaned, the growth of single crystals may commence. The seed is strongly attached to the seed shaft by securing a 1 mm. diameter molybdenum wire around the seed grooves and the shaft grooves. Provided the shaft and seed are properly mounted to the lifting mechanism, the cleaned Ge may be placed into the graphite and fused silica crucible. Prior to sealing the crystal grower it is a good precaution to ensure that the seed rotation and lifting mechanism are functioning properly. Fig A illustrates the attached seed and polycrystalline Ge. Crucible rotation can also be started to ensure that rotation is concentric about the graphite heater. Centering of the crucible is necessary to provide uniform heat distribution to the charge. Provided all mechanical

operations are functional, the crystal grower bell jar may be sealed to the growth chamber and pumping down may commence.

Evacuation of the growth chamber is accomplished by a mechanical roughing pump. Pumping down to a pressure of 1.3 Pa. is performed in approximately 20 minutes. The removal of any moisture that could have collected on the chamber surfaces or on the Ge, is done by purging the chamber with high purity argon gas. The purging process is repeated three times.

The growth of any semiconductor crystal may take place in either a vacuum or inert gas environment. To eliminate the possibility of any rotary pump oil backstreaming into the growth chamber, it was decided that crystal growth should be performed in an argon gas environment. The delivery pressure of the gas is set to 68.9 kPa with a gas flow restricted to 15 scfm. To prevent any gasket ruptures due to gas pressures, a bleeder valve and trap assembly was affixed to the growth chamber. The purpose of the trap is to prevent any back diffusion of the external gas into the growth chamber.

Temperature measurements during all phases of the growing process are accomplished by a radiomatic pyrometer positioned to sense the energy emitted by the bottom of the graphite crucible. The pyrometer generates a millivoltage proportional to the crucible temperature and is used as a primary signal while in the automatic mode.

In addition to being connected to the power controller, the pyrometer is also monitored by a 5½ digit high impedance voltmeter. The purpose of the voltmeter is to provide the operator with an approximate range or voltage at which the Ge starts to become molten. Once the temperature of the crucible is within 150°C of the melting point, the chart recorder is activated to graphically illustrate the process temperature. The chart recording of the temperature provides indications of how the power controller and process controls are functioning. If no abnormalities are noticed, the power controller is switched from the manual to automatic mode. Fig B illustrates the heating up of the Ge charge. The purpose of the automatic mode is to ensure that the temperature of the crucible does not deviate more than ± 0.5 °C from the desired setpoint. To achieve this accuracy as well as selecting the process controls to allow the grower to respond to temperature changes, tuning of the three process controls must be effected.

Since the crystal grower is acting as a closed loop feedback system, tuning of the process controls to minimize temperature overshoot and reaction time must be performed. The controls to effect this are proportional band, reset and rate time. The function of these is to operate upon the error voltage generated by the difference in actual and setpoint temperatures. In addition to these process controls, there exists a programmer / controller. This feature makes it possible to motor drive the setpoint either upscale or downscale at a preset rate. This becomes useful for ramping the temperature of the melt at certain times during crystal growth.

Depending upon the melt temperature three possible situations exist. If the temperature of the surface is correctly determined, the seed will cool it sufficiently to start the nucleation of solid Ge onto the seed, thereby increasing the crystal mass. If the melt temperature is too hot and the seed is immersed, the net heat flux will melt away the seed and once the pulling is initiated, the seed will separate from the melt. If the temperature of the melt is too cool and the seed has been immersed, the effect of the seed will be to cool down the melt extremely fast, thereby making the aspect of a controlled freezing very difficult to achieve. Since no absolute indication of the melt temperature is provided, an alternative method must be used prior to the seeding action. Initially the melt is held at a temperature slightly higher than its melting point. It is left at this temperature for several minutes to eliminate any possible temperature lag. Using the programmer the melt temperature is decreased very slowly. The melt is constantly viewed for the formation of solid material on the surface of the melt, usually appearing in the form of an island. Once it has appeared, it indicates that the melt is near to the seeding temperature. The temperature of the melt is increased a few degrees and the seed is lowered to within 1.0 cm of the surface to preheat it prior to immersion.

Provided the temperature of the melt is properly determined, the next task is to start the pulling of the crystal from the melt. Since the temperature has been properly determined, the seed is immersed

approximately 6mm. into the melt. This is illustrated in Fig C. The purpose of this step is to allow the surface heat to melt a small portion of the seed, still leaving the core intact. This nucleation step is one of the most crucial, since it is at this phase that the crystal orientation is duplicated. Under certain conditions, the growing process may be continued, however the orientation will change. This phenomena is known as crystal twinning.

The seed is left immersed in the melt for 5 to 7 minutes. This allows ample time for the seed to sufficiently cool the solution about it. Once the seeding is completed, the mechanical aspects of crystal growing may be initiated. Crucible rotation is started (set to 20 RPM) to ensure uniform heat distribution to the crystal. Thorough mixing of the melt is performed by seed rotation (set to 10 RPM). Of course seed pulling is started to commence the growth of the crystal (set to 2.5 cm/hr).

Crystal growth during the next 30 minutes is crucial for several reasons. In the initial stages the diameter of the newly formed crystal must be controlled. Crystal orientation information will be revealed during the early stages of growth. If at any time the operator believes that the orientation is improper, the partially grown crystal may be reinserted into the melt and the growth recommenced. Provided the nucleation is successful, the next step is to ensure that the "neck" of the crystal is properly grown.

The "neck" of the crystal is that portion of the crystal directly below the seed and extends approximately 2.0 cm. in length. Fig D illustrates the formation of the "neck". To minimize the propagation of dislocations it is important to maintain the diameter of the "neck" very close to that of the seed. It is hoped that any dislocation formed during the creation of the "neck" may grow outwards, leaving the crystal at an early stage. Owing to the thinness of the "neck", no direct sign of crystal orientation is visible. Once the length of the "neck" is sufficient, the growth of the "shoulders" may commence.

Since the diameter of the crucible is 8.9 cm. the crystal diameter is restricted to 6.4 cm. The growth of the "shoulders" is accomplished by allowing the solid-liquid interface at the melt surface to slowly grow outwards to the crucible wall. This is accomplished by using the programmer, and changing the pull rate of the crystal grower. The "shoulders" are created by increasing the rate of temperature decrease as well as decreasing the pull rate. Fig E illustrates the shoulder formation. The time required to grow the "shoulders" is approximately 20 minutes. The only precaution to observe is to avoid having the solid/liquid interface reach the crucible wall. Experience has shown that if the "shoulders" are grown gradually, the possibilities of dislocation formation are minimized. The length of the "shoulders" are approximately 1.9 cm.

Once the "shoulder" size is considered adequate, the programming of the diameter must be changed in order to form the crystal body. As would

be expected, the growth of the body is affected by lowering the rate of temperature change and increasing the pull rate. By increasing the pull rate the diameter will decrease since crystal mass is being cooled at a faster pace. An equilibrium will be reached whereby the two controls produce an isotherm at the solid-liquid interface. Therefore, by properly controlling both parameters, the diameter of the body may be formed. The total length of the body can be approximately 7.6 cm. The length is dependent upon diameter size and charge weight. The time required to grow the body is approximately 3 hours. Fig. F and G illustrate the growth of the body.

Several of the first crystals grown had large variations in their body diameters. Their appearance is typical of improper adjustment of the growing controls. Fig. H illustrates such a crystal. However with experience and "feeling" for the sensitivity of the programming control and pulling rate, proper crystals were grown. Because the melt temperature is constantly decreasing for the entire duration of the growing, a time will be reached at which the temperature of the melt will be cool enough to solidify the remaining melt in the crucible. It is important to observe for this occurrence, for if the solidification of the crystal is allowed to attach itself to the crucible wall, the possibility of the crystal detaching from the seed shaft does exist. This scenario is to be avoided since the seed may crack and become unusable for future growing sessions. To eliminate this possibility it was advisable to increase the temperature of the melt near the end of the growth. This has the effect of decreasing the diameter of the crystal. Figures I and J il-

lustrate the completed growth of the crystal. Table 3.1 illustrates several of characteristics and comments associated with the crystals grown in the laboratory.

CRYSTAL	SUCCESS	COMMENTS
#1 <111>	N	(a) The melting point of the melt was determined. (b) The effect of the process parameters was investigated. (c) Observed the formation of oxides on the surface ofthe melt. (d) At the end of the growth, the crystal attached itself to the crucible, thereby detaching itself from the seed shaft.
#2 <111>	N	(a) Five crystal faces were observed instead of the expected six. This is indicative of twinning. The growth was finished as a practice excercise.
#3 <111>	Y	(a) The resulting crystal had a diameter of 6.9 cm. The pulling rate was set to 2.5 cm/hr. The operation of extracting the seed and a small disk was performed to illustrate that it was a single crystal. (b) The results of the crystal are demonstrated as sample No. 1 in Table 3.1.
#4 <111>	N	(a) While awaiting for the arrival of the <100> seed, another attempt at growing a crystal was performed. The operation had to be aborted since it was discovered that the infrared transparent window of the radiomatic pyrometer had a fine layer of grease covering it. The source of this contamination was discovered and the problem was rectified.

Table 3.1 (continued)

#5 <100>	Y	(a) Using the <100> seed, a crystal with a diameter of 6.4 cm. and length of 8.5 cm. was grown. It illustrated the four-sided structure common to a <100> crystal. (b) The results of the crystal are shown as sample No.2 in Table 3.1
#6 <100>	Y	(a) Once all the practice of undoped crystals were performed, Dr. Lombos suggested that doping may commence. (b) An ampoule was prepared and its contents were melted to create a doping alloy. (c) A doped crystal was grown with a diameter of 5.9 cm. and a length of 8.5 cm. (d) Hall-Effect samples were extracted at two locations along the crystal. The results of this analysis is reported as sample No. 4 and 5.
#7 <100>	Y	(a) A second crystal was grown. It followed the same procedure as run #6. The crystal had a diameter of 5.5 cm. and a length of 8.0 cm. (b) Hall-Effect samples were extracted and the analysis is represented as samples No. 6 and 7 in Table 3.1

Table 3.1 Characteristics and comments of the crystals grown.

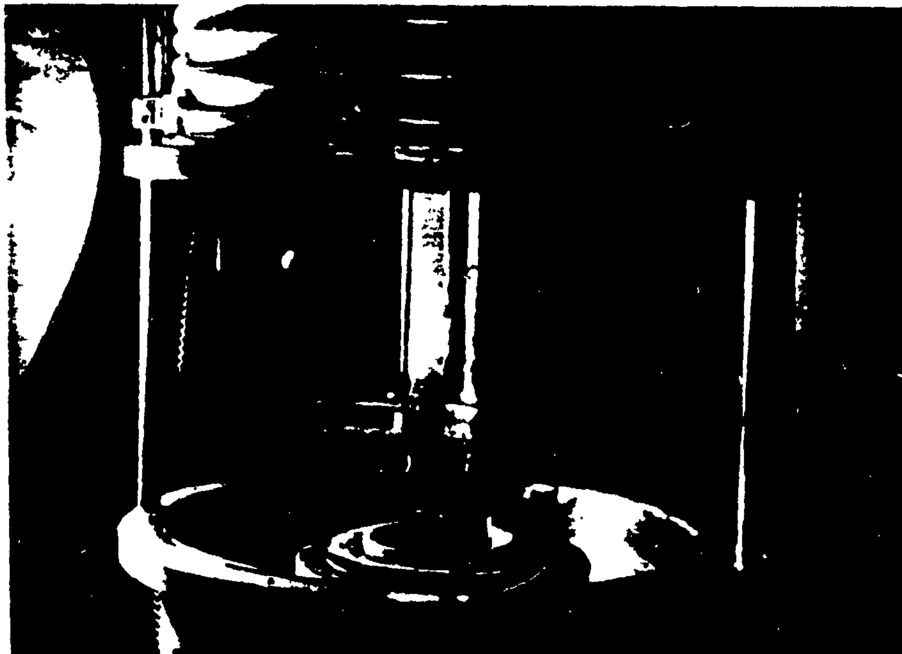

Fig A. Seed mounted to shaft and Ge charge placed into crucible.

Fig B. Heating of charge to molten state.

Fig C. Seed is touched to surface of melt.

Fig D. Formation of "neck" is finished.

Fig E. "Shoulder" formation is nearing end.

Fig F. Half of the body is completed.

Fig G. Close to completing the full growth.

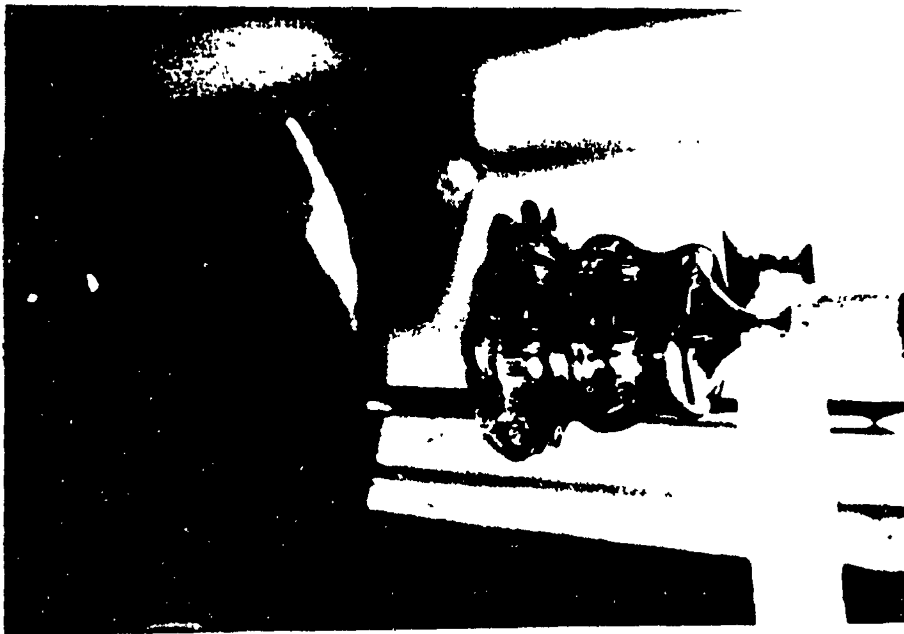

Fig H. Grown crystal illustrating improper process control.

Fig I. Crystal mounted on shaft after cooling period.

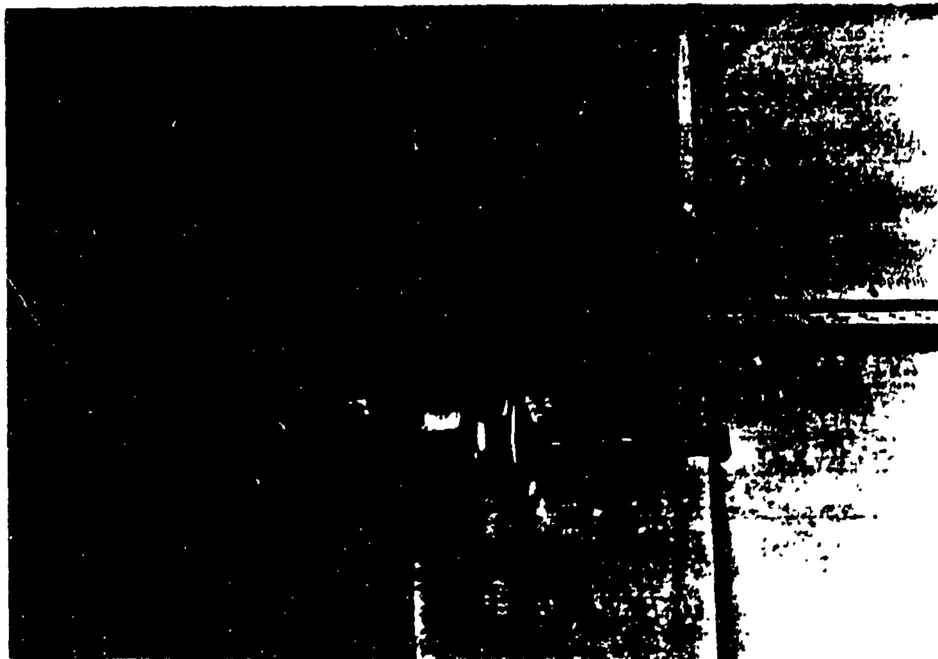

Fig J. Profile of 2.5 inch Ge crystal.

3.3 CREATION OF A DOPING ALLOY

Since the purpose of the Ge is to act as a suitable substrate for GaAs deposition for the creation of high efficiency solar cells, it was decided that the following crystals should be doped. Owing to the structure of the solar cell and the creation of minority carriers in the thin GaAs layer, the dopant for the Ge was chosen n-type. Several dopants could be used, all of which are group V elements, namely P, As or Sb. Owing to its ease of handling and relative lack of toxicity, antimony, Sb was chosen. Eventhough Sb and As are classified as poisonous (Sb has a TLV (Threshold Limit Value) of 0.5 mg/m^3 and As has a TLV of 0.2 mg/m^3), their physical properties at the melting point of Ge are quite different. Antimony exhibits a vapour pressure of 1 mm at its melting point of 886°C, whereas As sublimes at 612°C and at its melting point has a vapour pressure of 36 atm. Therefore one may conclude that Sb will remain in the melt, whereas As would recondense on the cooler parts of the growth chamber or escape via the N_2 bleeder system, making it unsuitable as a dopant.

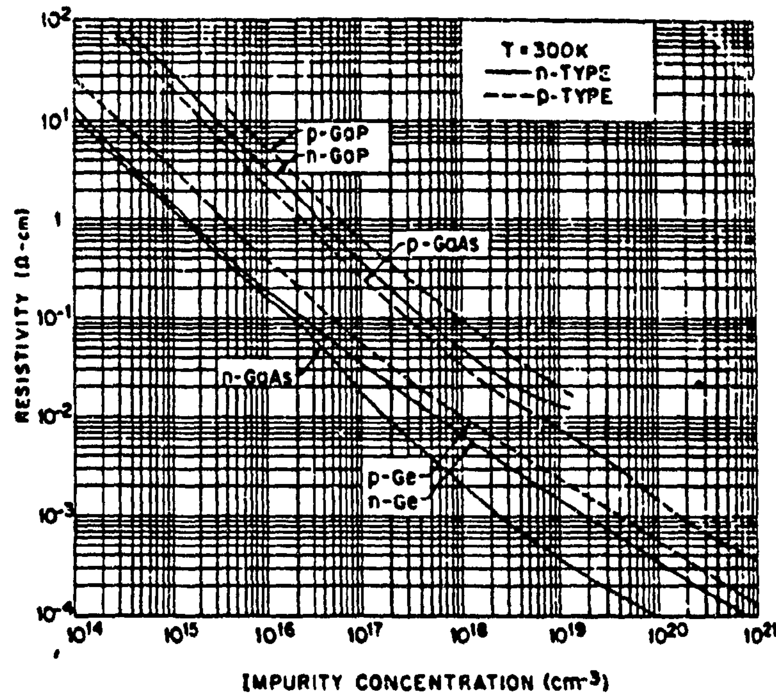

Fig 3.1 Graph illustrating concentration vs resistivity[29]

The resistivity of the Ge was decided to be in the range of 0.1Ω-cm. From the graph shown in Fig. 3.1, it can be seen that the carrier concentration of the dopant should be approximately 2 x 10^{16} at/cm^3.

One may ask themselves if this amount of Sb may be added directly to the charge. Appendix A illustrates the amount of Sb required to achieve this doping concentration.

Since a minute quantity of Sb is very difficult to measure accurately, the alternative is to create a doping alloy. The purpose of the doping alloy or doping pellet is to use a small quantity of Ge as a

solvent, and thoroughly saturate this semiconductor material with Sb until it reaches its maximum solid solubility.

The Sb concentration can be determined, as well as the number of Sb atoms per unit mass of the alloy. A small amount of this doping alloy, corresponding to the required melt concentration, usually 30 - 40 grams can easily be added to the Ge charge with the assurance that the doping concentration (C_o) is close to that desired.

A closed evacuated ampoule system was used to create the doping alloy. Several attempts were made by using an open ampoule system. However, it was soon discovered that the antimony sublimated at approximately 600°C at a vacuum of 1.33 x 10^{-3} Pa. present within the evaporator. Energy is supplied in a radiative fashion by the heating of a tungsten filament.

Therefore, to eliminate the escape of Sb, an evacuated closed ampoule was used. This technique is very similar to the growth of crystals by the Horizontal Bridgman method. A fused quartz ampoule and endcap were made by the glassblower with the specification that its length not exceed 7.6 cm. The ampoule was then cleaned and etched as described earlier for the crucible. The raw Ge was also cleaned. The antimony shot used indicated a 5n (99.999%) purity. The Ge which is ap-

proximately 50 grams is placed into the ampoule with enough Sb shots, approximately 15 pieces, to saturate. The ampoule with its contents are then fused to its endcap. Provided the fusing is sufficient to be airtight all that remains is to evacuate all air from within. The evacuation tube connected to the endcap is attached to the vacuum system. Under the best conditions, the vacuum within the ampoule can be reduced to 1.33×10^{-3} Pa. This is the best for the available diffusion pump and liquid nitrogen cold trap.

The ampoule is now prepared for its contents to be melted. The ampoule is placed horizontally within the graphite crucible in the crystal grower. It is positioned horizontally to minimize the temperature gradients present in the crucible.

The creation of the doping alloy follows the same procedure of heating the Ge during the crystal pulling. The melting temperature is reached relatively fast within approximately 60 minutes and then slowly cooled in approximately 120 minutes. The heating procedure of the doping alloy is very similar to that of crystal pulling.

Once the ampoule has cooled sufficiently, the doping alloy is extracted by carefully cracking the opposite end of the ampoule. The doping alloy is then withdrawn and placed in a clean environment. Appendix B illustrates the amount of doping alloy that is required.

CHAPTER IV

EXPERIMENTAL RESULTS

4.1 PREPARATIONS PRIOR TO ANALYSIS

To ascertain any physical characteristics of a grown crystal such as dopant concentration, dislocation density, and crystal orientation, several preliminary steps must be performed.

The crystal must be mounted on a slicing block to allow the wire saw to cut entirely through. The crystal is mounted in melted wax, then secured and aligned in the wire saw. The alignment is performed by eye to ensure that all cuts are as close to perpendicular as possible to the longitudinal axis of the crystal (the <100> direction). The first cut into the crystal is performed to liberate the seed, thereby eliminating any accidental damage to it. This cut is done at a location where new crystal material is grown, since it is the orientation of the new crystal which is of interest. Fig. 4.1 illustrates the seed separated from the crystal.

Proceeding from the removal of the seed, a small disk is then extracted from the crystal. The disk thickness is chosen to be 1.5-2.0 mm. This j chosen for the following reasons:

1- This disk is used to ascertain whether the crystal is single

or not. Therefore a comfortable thickness is chosen to lap.

2- If the crystal is single, it may be used for either Hall-Effect, dislocation density or X-ray diffraction analysis.

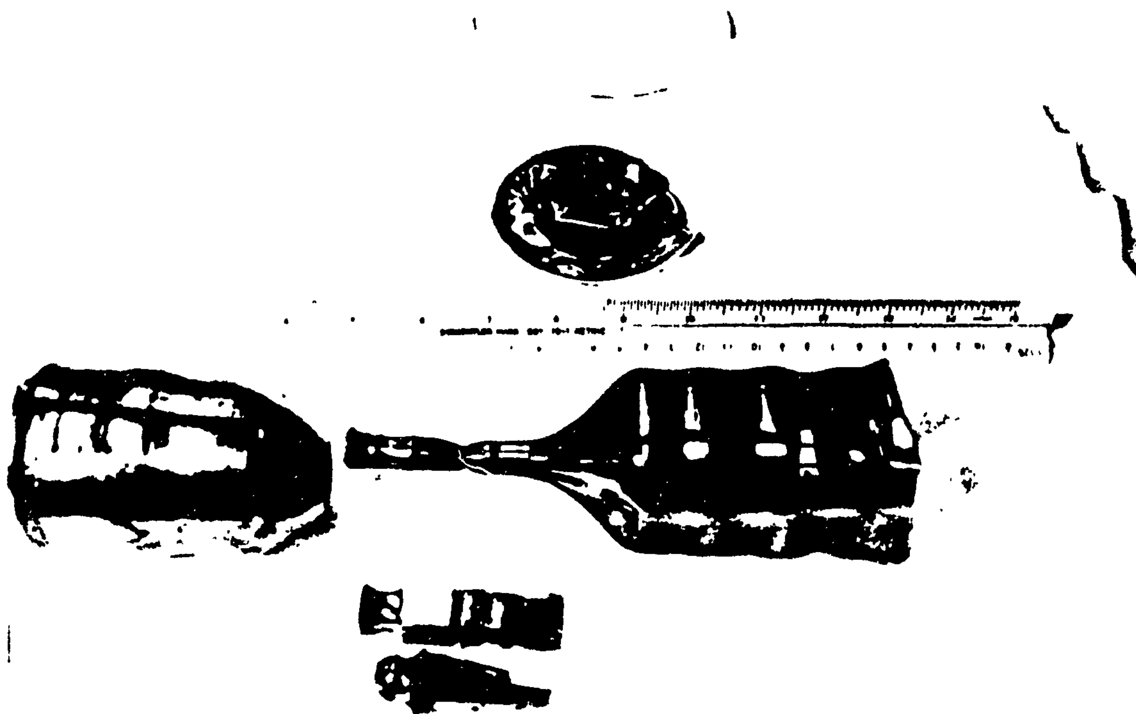

Fig 4.1 Seed removed from grown crystal

In order to determine if the crystal is single crystal, it is necessary to rough grind the disk with a coarse 220 grit SiC abrasive. This is followed with a smoother 50 micron alumina powder. All grinding/polishing is done on a smooth glass plate and requires 20 - 30 minutes. Once the surface is adequately matte, room light is reflected off the surface. If two or more distinct planes are seen then a difference in crystal orientation is evident.

Provided the crystal is single crystal, the small disk may be used as a Hall-Effect sample. The location of the disk is then recorded as a fraction of the entire length of the crystal to relate to the segregation coefficient analysis (see eqn [2.1]). The disk is lapped to a thickness of approximately 1.0 mm. This thickness must be uniform and known accurately, and therefore is measured with a vernier.

Hall-Effect bulk samples can be measured either by a 6 point or 4 point measurement setup.[30] A convenient tool to execute a 6 point analysis is a miniature sandblasting glove box and a 6 point replicating steel mask.

Initially, the disk is polished on both sides. To create the 6 point sample, the disk is wax mounted onto a steel plate. Once the disk is securely placed, more molten wax is poured onto the top of the disk. The 6 point mask is then carefully placed and centered onto the disk. The entire plate/disk/mask ensemble is then left to cool and harden.

The sandblaster is powered by nitrogen or argon gas at a delivery pressure of 345 - 415 kPa. An inert gas is used to prevent the samples from oxidizing. The sample is then placed into the sandblaster. A fine nozzle is provided to ensure that the sand hits the Ge at a 90° angle. This is performed to minimize the sidewall angle of the sample.

A typical bridge-type sample, which is obtained by sand-blasting,

is shown in Fig. 4.2. Also illustrated are the voltages measured to calculate the resistivity of the sample.

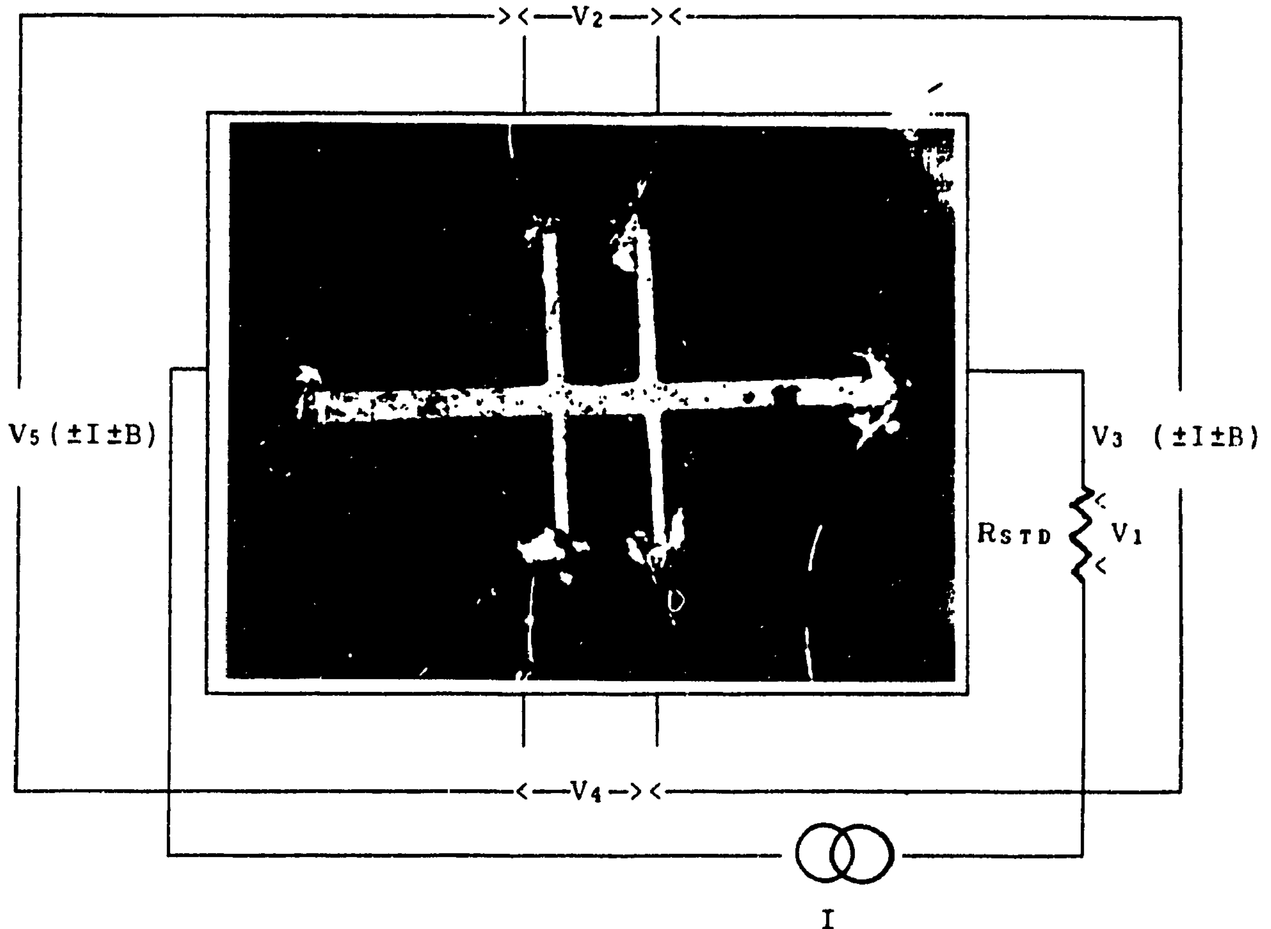

Fig 4.2. Hall sample indicating current and voltage terminals

Cleaning of the sample is done by boiling in trichloroethane, acetone and methanol several times for 15 minutes. The purpose of this is to remove any of the mounting or sandblasting material which may affect the voltages acquired during the analysis. The dimensions d (distance between leg electrodes), t_s (sample thickness) and w_s (sample

width) are accurately measured using either a travelling microscope or a vernier. Once these dimensions are recorded, soldering contacts and mounting the specimen may commence.

As suggested by the ASTM standard[31] for Hall-Effect analysis, indium solder is used to form an ohmic contact between the Ge and gold wires needed to measure the Hall voltages. The indium is applied by a soldering iron whose tip temperature is adjusted slightly higher than the melting point of indium. As the solder is applied, it must appear to cover as much of the leg area as possible. If the solder appears to "ball-up", bonding strength as well as the likelihood of a low ohmic contact are poor. Therefore the objective of the soldering is to achieve good coverage over the leg area. No flux is applied to eliminate any residues which may affect the electrical measurements. Once the solder application is completed, gold wire of length approximately 1 cm. and diameter < 0.5 mm. is gently melted into the solder. The quality of the solder is ascertained by applying a curve tracer between the bulk Ge and the solder contact. If the i-v characteristic yields a nonrectifying low ohmic resistance (approximately .6 - .8 Ω) the contact is determined to be appropriate for Hall-effect analysis. With the sample placed into the specimen holder, the remaining ends of the gold wire are then soldered to the appropriate pins on the specimen holder which are responsible for applying current to the sample and sensing the minute Hall voltages. The entire ensemble is then placed into a non-magnetic dewar, thereby eliminating ambient light. The direction of the sample is placed perpendicular to the magnetic field.

4.2 HALL-EFFECT MEASUREMENTS

Hall measurements are widely used in the initial characterization of extrinsic doped semiconductor materials to measure their carrier concentration and mobility. The evaluation of the Hall mobility requires the electrical resistivity and Hall coefficient to be determined. Therefore mobility determination provides an opportunity to evaluate these properties separately.

Fig 4.3 illustrates a magnetic field applied perpendicularly (in the z axis) to the direction of hole current (in the x axis) in a p-type sample.

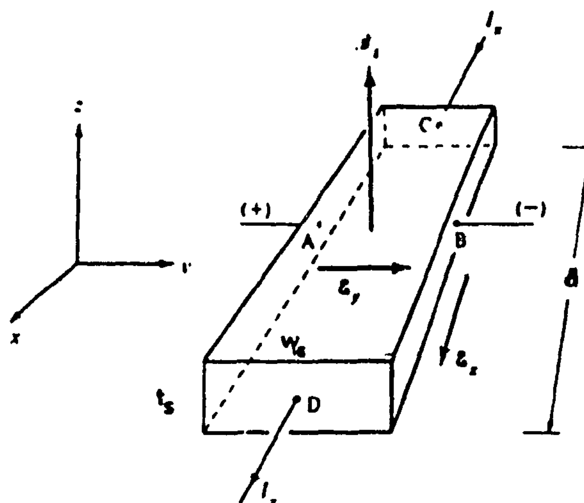

Fig. 4.3 Hall sample with external fields applied.

Under the external influences of an electric and magnetic field, the path of the holes tend to be deflected. The magnitude of the force exerted upon a hole in the y direction is given by[32] :

$$F_y = q(E_y - v_x \cdot B_z) \qquad [4.1].$$

where E_y is the electric field created by the redistributed charges.

v_x is the velocity in the x direction.

B_z is the applied magnetic flux density in the z direction.

q is the elemental charge (1.609 x 10^{-19} coulombs).

To maintain a constant current through the sample, the net force F_y should equate to zero. Therefore

$$E_y = v_x \cdot B_z \qquad (V/cm) \qquad [4.2]$$

and the voltage V_H which produces this field E_y is simply

$$V_H = E_y \cdot w \qquad (V) \qquad [4.3].$$

The voltage, V_H across the bar sample, is termed as the Hall voltage. Intuitively the formation of the Hall field, E_y, is caused by a redistribution in the hole concentration created by the application of the magnetic field B_z.

Thus the Hall field is proportional to the product of the current density J_x and the magnetic flux density B_z. The proportionality constant is the Hall coefficient $R_H = (q\ p_0)^{-1}$, where p_0 is the hole concentration.

More elaborate theory predicts that[33]

$$R_H = \frac{-r_n}{nq} = \frac{r_p}{pq} \quad (cm^3/C) \qquad [4.4].$$

where $r_{n,p}$ is a constant, usually between 0.5 and 1.5 and usually depends on the specific details on conduction in the material. For the conduction of a semiconductor whose energy bands are spherical, r can be equated as[34]

$$r_n = r_p = \frac{3\pi}{8} \qquad [4.5].$$

By making measurements at high enough magnetic field, r can be reduced to 1, regardless of the conduction process. Since the procedures to determine the carrier concentration are performed according to ASTM (American Society for Testing and Materials) specifications, all assumptions herein should be identical to those made in this specification. Since a detailed knowledge of the proportionality factor r in Ge is not known, all users have agreed to equate r to unity. In any event, the error introduced by determining n directly with no prior knowledge of r is not large.

A measurement of the Hall voltage for a known current and magnetic field yields a value for the hole concentration p_0 as

$$p_o = \frac{1.0}{q\ R_H} = \frac{J_x \cdot B_z}{q\ E_y} \quad cm^{-3} \qquad [4.6].$$

Since all the quantities in the right-hand side of eqn[4.6] can be measured, the Hall effect can be used to give quite accurate values for carrier concentrations. The sample resistivity p can be calculated as:

$$p = \frac{V \cdot w_s \cdot t_s}{I_x \cdot L} \quad \Omega - m \qquad [4.7]$$

Where V is the voltage created by the application of the external current, I_x. The Hall mobility is simply the ratio of the Hall coefficient and the resistivity. The fact that the carrier concentration can be determined with no prior value of r, and the relatively easy use of Hall measurements have accounted for its widespread usage and adoption as a standardized semiconductor test method, namely ASTM F76.[35]

4.2.1 HALL-EFFECT MEASUREMENT PRECAUTIONS

The techniques of determining the Hall mobility of a semiconductor are quite straight forward, however certain precautions which are outlined in the ASTM procedures should be observed. In making resistivity and Hall-Effect measurements, spurious results can arise from a number of sources.

1) Photoconductive and photovoltaic effects can seriously influence the observed resistivity, particularly with nearly intrinsic material. Measurements should be made in a dark enclosure.[35]

2) Minority - carrier injection can occur because of the electric field in the specimen. With materials possessing high minority-carrier lifetime and resistivity, such injection can result in a lowering of the resistivity for a distance of several millimeters along the bar. Carrier injection can be detected by repeating the measurements at lower applied voltages. In the absence of injection no increase in resistivity should be observed.[36]

3) Semiconductors have a significant temperature coefficient of resistivity. Thus the temperature of the specimen should be known and the current used should be small enough to avoid resistive heating.

4) Inhomogeneities of the specimen impurity distribution or of the magnetic flux will cause the measurements to be inaccurate.

4.2.2 RESISTIVITY DETERMINATION

The resistivity of a semiconductor is a directly measurable quantity and is indicative of the materials ability to conduct charge carriers. Experimentally the resistivity of a 6 point sample is determined as:[37]

$$\rho_a = \frac{1}{2}\left[\frac{V_2(+I)}{V_1(+I)} + \frac{V_2(-I)}{V_1(-I)}\right] R_{std}\, w_s\, \frac{t_s}{d} \qquad [4.8]$$

The parameters $V_2(+I)$, $V_2(-I)$, $V_1(+I)$ and $V_1(-I)$ are the measured voltages indicated in Fig 4.2. The variables +I, -I indicate positive and negative current directions respectively. The units of voltage are arbitrary but the same. The standard resistor R_{std} is measured in ohms, and all dimensions w_s, t_s, d are in cm. A second resistivity, ρ_b, is evaluated with voltages $V_4(+I)$ and $V_4(-I)$ replacing $V_2(+I)$ and $V_2(-I)$. The sample is deemed inhomogeneous if ρ_a and ρ_b differ by more than $\pm$10%.

4.2.3 HALL COEFFICIENT DETERMINATION

The Hall coefficient is also experimentally attainable, and is a measure of the concentration of charge carriers. It is determined by the following formula:[38]

$$R_H = \frac{1}{4}\left[\frac{V_3(+I,+B)}{V_1(+I,+B)} + \frac{V_3(-I,+B)}{V_1(-I,+B)} - \frac{V_3(-I,-B)}{V_1(-I,-B)} - \frac{V_3(+I,-B)}{V_1(+I,-B)}\right] R_{std}\frac{t_s}{B} \qquad [4.9]$$

The independent variables +I, -I, +B and -B represent positive and negative directions of current and magnetic flux respectively. The units are identical to that of resistivity with the magnetic flux B, measured in gauss. The coefficient has the characteristic of being negative for n-type material and positive for p-type material. The second coefficient (R_{H5}) is simply determined by replacing the V_3 voltages with the V_5 voltages indicated in Fig 4.2. If the two coefficients differ less than 10% the average coefficient may be considered representative of the sample.

4.2.4 SAMPLE CALCULATION

The following are typical data that was acquired during a resistivity and Hall coefficient determination. The data for the resistivity and mobility measurement are the following:

R_{std} = 1160 Ω	$V_1(+I)$ = 1.160 v	$V_1(-I)$ = -1.160 v
d = 0.293 cm	$V_2(+I)$ = 0.2109 v	$V_2(-I)$ = -0.2261 v
t_s = 0.10 cm	$V_4(+I)$ = 0.2214 v	$V_4(-I)$ = -0.2302 v
W_s = 0.31 cm		
B = 5000 gauss		
I = 1.00 mA		
temp.= 23.0 °C		

The data gathered to determine the Hall coefficient appears as follows:

$V_1(+I,+B)$ = 1.160 v	$V_1(-I,+B)$ = -1.160 v	$V_1(-I,-B)$ = -1.160 v	$V_1(+I,-B)$ = 1.160 v
$V_3(+I,+B)$ = -.0250v	$V_3(-I,+B)$ = .0289 v	$V_3(-I,-B)$ = -.0772 v	$V_3(+I,-B)$ = .0776 v
$V_5(+I,+B)$ = -.0650v	$V_5(-I,+B)$ = .0678 v	$V_5(-I,-B)$ = -.0245 v	$V_5(+I,-B)$ = .0224 v

Using the above data the resistivity ρ_a is determined as follows

$$\rho_a = \frac{1}{2}\left[\frac{.2109}{1.160} + \frac{-.2261}{-1.160}\right]\frac{(1160)(.31)(.10)}{.293}$$

$$= 23.11\ \Omega\text{-cm.}$$

And the second resistivity calculation follow as:

$$P_b = \frac{1}{2}\left[\frac{.2214}{1.160} + \frac{-.2302}{-1.160}\right]\frac{(1160)(.31)(.10)}{.293}$$

$$= 23.89 \quad \Omega\text{-cm}$$

Therefore $P_{ave} = 23.50 \quad \Omega\text{-cm}.$

The Hall coefficient calculation is determined by the following calculation:

$$R_{H3} = 2.5\text{x}10^{7}\left[\frac{-.0250}{1.160} + \frac{.0289}{-1.160} - \frac{-.0772}{-1.160} - \frac{.0776}{1.160}\right]\frac{(1160)(.1)}{5000}$$

$$= -\ 104347.8 \ \text{cm}^3/\text{C}.$$

The second coefficient is determined by the same means as the above calculation. It is computed as:

$$R_{H5} = 2.5\text{x}10^{7}\left[\frac{-.0650}{1.160} + \frac{.0678}{-1.160} - \frac{-.0245}{-1.160} - \frac{.0244}{1.160}\right]\frac{(1160)(.1)}{5000}$$

$$= -\ 89842.0 \ \text{cm}^3/\text{C}.$$

Therefore the average Hall coefficient is determined as -

$$R_{Have} = -97094.5 \quad \text{cm}^3/\text{C}.$$

From these two results, the impurity concentration is determined as:

$$n = \frac{1}{(97094.5)\ (1.6 \times 10^{-19})} = 6.45 \times 10^{13} \ \text{cm}^{-3}$$

and the mobility is determined as:

$$\mu = \frac{R_H}{P_{ave}} = \frac{97094.5}{23.50} = 4131.7 \ \text{cm}^2/\text{V}\cdot\text{s}.$$

The following are the Hall-Effect results for samples 1 - 7:

SAMPLE	ORIEN-TATION	P(Ω-cm)	R_H (cm^3/C)	conc(cm^{-3})	μ ($cm^2/V\cdot s$)
1	<111>	23.50	97094.5	6.45×10^{13}	4131.7
2	<100>	22.12	88712.6	7.1×10^{13}	4010.6
3	<100>	.00864	11.02	5.69×10^{13}	1275.1
4	<100>	.726	2917.5	2.15×10^{15}	4016.5
5	<100>	.150	498.76	1.25×10^{16}	3324.1
6	<100>	.667	2396.4	2.61×10^{15}	3592.8
7	<100>	.146	416.6	1.5×10^{16}	2849.4

Table 4.1 Characteristics of the crystals grown

4.2.5 COMMENTS OF RESULTS

SAMPLE (1)

A crystal was grown using an available <111> seed to ascertain how well the crystal grower functions, and if so to become familiar with its process controls. The resulting crystal illustrates a high resistivity measurement. This is indicative of very little impurity contamination which could possibly occur from either the grower or during material handling.

SAMPLE (2)

After many hours of familiarity and acquiring confidence of growing several crystals, a <100> seed was purchased. Substrates oriented in this direction are the preferred crystal planes for subsequent epigrowth. The <100> crystal showed electrical properties very similar to sample (1).

SAMPLE (3)

Since the substrate material must be doped, a doping alloy was fabricated as described earlier . A small (≈ 45 grams) test ingot was frozen with a saturating amount of Sb. The low resistivity and high carrier concentration indicates the level of doping achieved.

SAMPLE (4)

A doped crystal was grown using a prescribed amount of the doping alloy evaluated in sample (3). The purpose of the alloy is to dope the crystal to a certain impurity concentration. The resistivity is close to

that which was designed ≈ 0.5 Ω-cm. Furthermore the fraction solidified (g=.1) versus impurity concentration was recorded to ascertain the segregation coefficient.

SAMPLE (5)

An identical analysis was performed on the same crystal in sample #4, however at a different location (g=.85). By the difference in the impurity concentration, the segregation coefficient is evidently < 1.

SAMPLE (6)

A second crystal was grown using the identical procedure as the previous crystal. Results would indicate that the concentration of the resulting crystal is somewhat off. The value of g at this point is .095. This indicates that some error is always present in any or all the steps required to perform this elaborate technique of producing doped semiconductor slices.

SAMPLE (7)

The same crystal was examined, however at a different location (g=.87). This was performed to determine the segregation coefficient for this crystal using almost identical growing conditions as the first doped crystal. The coefficient is again seen to be < 1.

4.3 DETERMINATION OF THE SEGREGATION COEFFICIENT

The effective segregation coefficient may be experimentally determined for a particular crystal growing experiment. The normal freezing equation presented earlier assumes that normal freezing occurs slowly and the solute concentration in the liquid is uniform. Under these conditions the freezing solid has a solute concentration K_o times that in the liquid, where K_o is the equilibrium distribution coefficient. However, when freezing does not occur slowly; as in Czochralski growth, the advancing solid rejects ($K < 1$) solute more rapidly than it can diffuse throughout the remaining volume of the liquid. Fig 4.4 illustrates the solute distribution in the vicinity of the solid-liquid interface. Therefore an enriched layer of solute concentration accumulates below the interface. It is the solute concentration in this layer, rather than that in the main body of the liquid, which determines the concentration freezing out in the solid.[39]

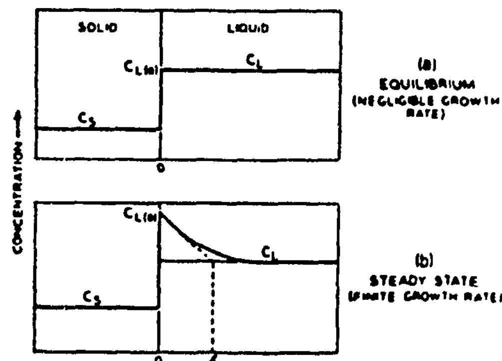

Fig. 4.4 Solute concentration at the solid-liquid interface.[40]

Hence under crystal growing conditions the relationship between concentration in the solid, C_s, and that in the main body of the liquid, C_L, can be described by an effective distribution coefficient, K_{eff} which equals C_s / C_l.

The experimental determination of the effective distribution coefficient involves the growth of a doped Ge single crystal by normal freezing. The solute concentration, C, is then determined by Hall-Effect analysis. The concentration is determined as a function of the fraction solidified X. The concentration is plotted against the fraction solidified; and compared against several other freezing curves. A logarithmic plot of the normal freezing equation is useful since it may be represented as a straight line. Thus if

$$\frac{C}{C_o} = K(1-X)^{K-1} \quad \text{then,}$$

$$\log \left[\frac{C}{C_o}\right] = \log K + (K-1)\log(1-X)$$

which has the form y = mx +b. Fig. 4.5 illustrates the graph of log(C/C_o) versus log(1-X). Both the slope and the intercept at (1-X) = 0 provide an accurate assessment of K_{eff} for the doped crystals grown under nearly identical growth conditions.

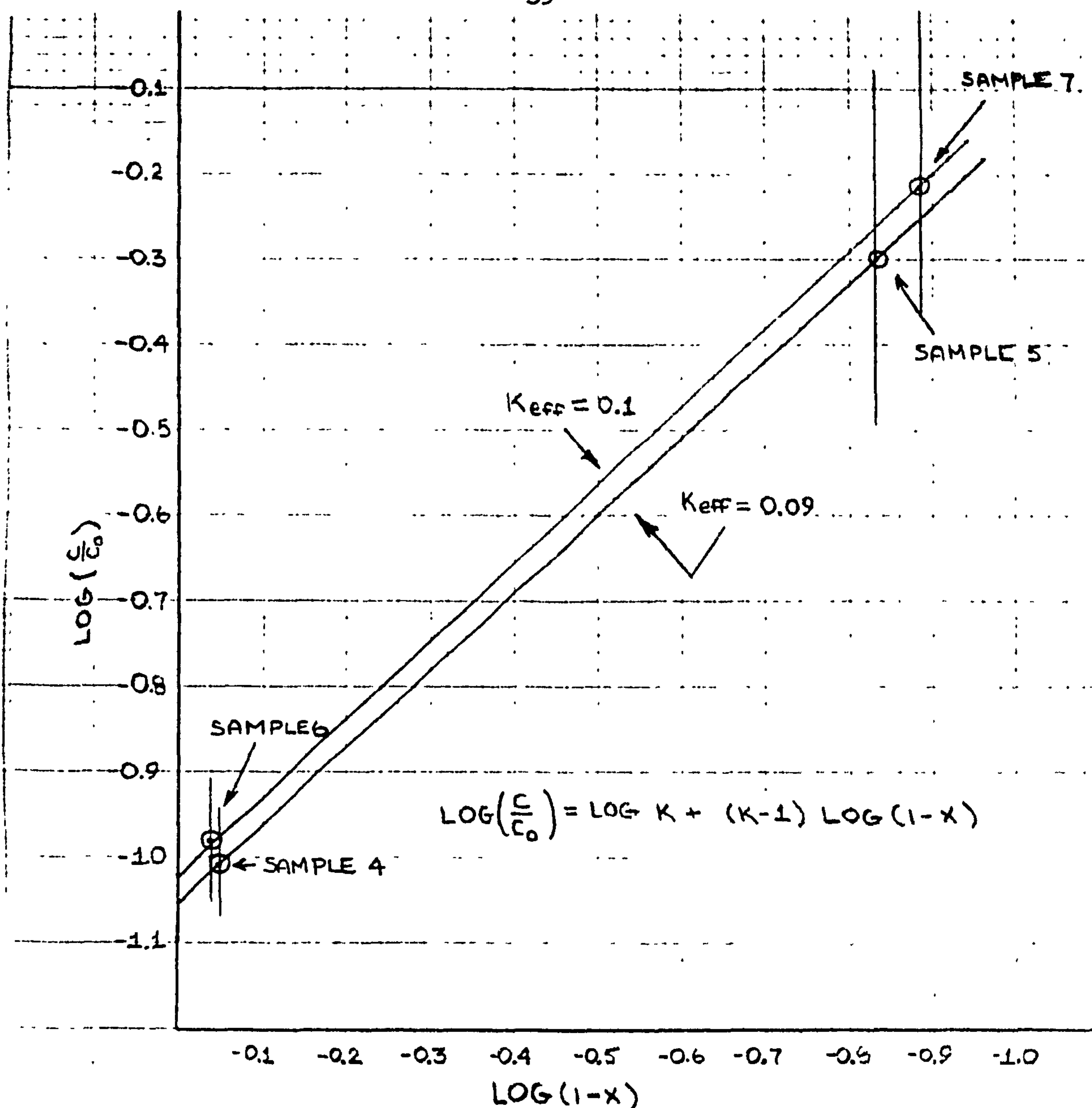

Fig 4.5 Plot of $\log(C/C_0)$ vs $\log(1-X)$ to determine K_{eff}.

From the plot it may be concluded that the effective segregation coefficient is approximately 0.1. Values of K_{eff} obtained by the slope and by the intercept differ. These differences are explainable by the errors in the course of experimental data acquistion as are indicated by the error bars for sample points.

Typically many data points must be acquired throughout the entire length of the crystal to determine K_{eff} with some degree of confidence. Fig. 4.5 illustrates only two points per line were determined. This was performed to allow the crystal to remain intact for future wafer production. Assuming, that the equation given in Fig. 4.5 is valid, the experimental points will lie on a straight line whose intersection with the ordinate determines K_{eff}. Following this procedure samples 3 and 4 resulted in $K_{eff} = 0.09$, whereas samples 6 and 7 yielded $K_{eff} = 0.1$.

4.4 DETERMINATION OF DISLOCATION DENSITY

The use of crystals in many semiconductor devices requires a periodic atomic lattice structure. If variations in structure, ie, imperfection sites, do exist, there will be a disturbance in the energy condition which is the basis for all semiconductor behavior. These dislocations have a distinct effect upon the processes of semiconductor diffusion and alloying.[41]

The technique of determining the crystallographic perfection of Ge by preferential etch is performed on a semiconductor slice which has been mechanically and chemically polished from the host crystal. The polished slice is then placed into an acid mixture which preferentially attacks the Ge in regions of crystal imperfection. The etched surface is examined microscopically to reveal the nature and extent of these imperfections. When a specimen is evaluated by this method with a specific etch compositions, dislocations are characterized by microscopic etched pits with pointed bottoms and planar sides.[42] Since these pits have sides which are not normal to the incident light, they will appear dark under vertical field illumination.

The chemical etchants and rinses required to reveal the dislocations are the following:[43]

CHEMICAL POLISH ETCHANT		
200 ml	Nitric Acid	(HNO_3)
120 ml	Hydrofluoric Acid	(HF)
100 ml	Acetic Acid	(CH_3COOH)
2 ml	Bromine	(Br_2)

<100> DISLOCATION ETCH		
500 ml	Hydrofluoric Acid	(HF)
500 ml	Distilled Water	(H_2O)
250 ml	Nitric Acid	(HNO_3)
25 g	Cupric Nitrate	$Cu(NO_3)_2 \cdot 3H_2O$

4.4.1 PROCEDURE FOR DEVELOPING ETCH PITS ON <100> Ge

The crystal should be oriented in the wire saw so that the surface to be exposed is within ½° of the <100> direction. Since this cannot be accomplished, the crystal ingot is positioned by eye to an angle which appears to be perpendicular to the orientation of the crystal. The cut sample should be at least 1.0 mm thick. Once the slice is extracted, the sample is mounted onto a lapping block. The lapping process is commenced with a No. 200 SiC grit. The surface must appear matte with no scratches, wax, or water stains. Areas of polycrystallinity are easily detected by a difference in light reflection. Mechanical polishing is completed by using successively smaller micron lapping powders.

Chemical polishing is performed after all mechanical polishing is completed. Approximately 100 ml of the polishing etchant is placed into a Teflon beaker. The etchant must cover the slice by at least 1.0 cm, and the lapped surface must be facing the etchant. After 2 minutes, the specimen has developed a chemically polished mirror surface, pour in distilled water to rapidly dilute and flush the etchant from the beaker. Pour off the rinse water and replace it with 30 to 50 ml of the dislocation etch. The dislocation etchant is allowed to etch the slice for 1.5 min at room temperature. The slice is then flushed with a nitric acid rinse (HNO_3 / H_2O 1:1 by volume). The slice is then rinsed with water

and nitrogen blown dried.

The specimen is then microscopically examined with a 20X objective to determine if the proper development of dislocation etch pits has occurred. Dislocation density is simply computed as the number of pits counted divided by the area of the field of view.[44]

To determine the area occupied by the dislocation pits a Scanning Electron Microscope (SEM) was used. A SEM is useful for two reasons (i) this form of an electron microscope is primarily a surface sensitive device capable of larger depth of field than an optical microscope, (ii) the SEM is capable of very accurate submicron geometry measurements, and hence will provide accurate dimensions of the field of view.[45] Fig 4.6 illustrates the micrograph of the dislocation pits.

From the SEM micrograph the total number of etch pits counted is 51. The dimensions of the field of view is provided by the micron bar. The area is simply .113 cm x .089 cm = 1.01×10^{-2} cm^2. Therefore the dislocation density is computed as

$$\text{dislocation density} = \left[\frac{51}{1.01 \times 10^{-2}}\right]$$

$$= 5049 \text{ dislocations / cm}^2$$

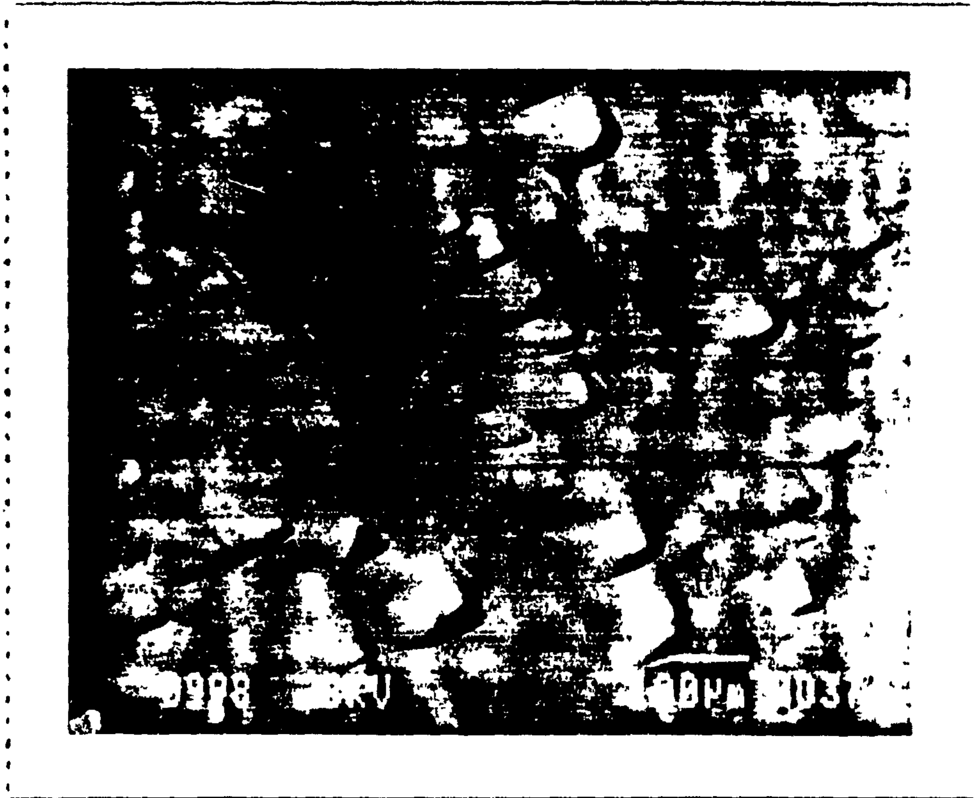

Fig. 4.6 SEM micrograph of dislocation pits

4.5 X-RAY DIFFRACTION

The determination of the crystallographic orientation of a semiconductor surface which is roughly parallel to a low index atomic plane may be ascertained by x-ray diffraction.[46] The orientation of semiconductor crystals is an important parameter since it has an influence on several semiconductor processes, e.g. homo- and heteroepitaxial growth.

The observation of x-ray diffraction is possible since atoms of a single crystal form a periodic three-dimensional array whose units may be visualized as lying in a series of parallel planes of equal perpendicular spacing d, as shown in Fig 4.7.

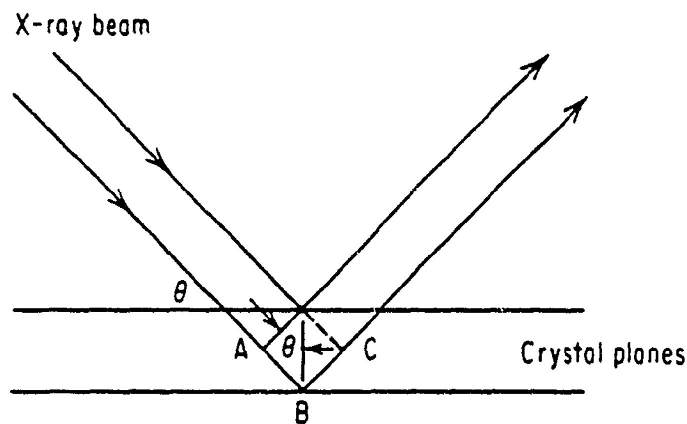

Fig. 4.7 Geometrical criteria for X-ray diffraction

When a collimated, monochromatic x-ray of wavelength λ is incident upon the semiconductor surface at an angle θ, a diffraction will occur

when the path difference of the x-ray between adjacent atomic planes is an integral number, n, of wavelengths. When this geometrical situation is present, the reflections from the various planes are exactly in phase and the diffracted beam is of maximum intensity. This phenomena is mathematically described as Bragg's law:[47]

$$n\lambda = 2d \sin \theta \qquad [4.10]$$

In semiconductor nomenclature, reflecting planes are commonly described in terms of their Miller indexes (h,k,l). The Miller indexes are formulated as being the smallest integers proportional to the reciprocals of the intercepts of the plane on the three unit crystal axes. Therefore, for any cubic lattice structure whereby the periodicity can be represented by a unit cell of side dimension a, the interplanar spacing d of a set of parallel atomic planes is simply:

$$d = \frac{a}{(h^2 + k^2 + l^2)^{\frac{1}{2}}} \qquad [4.11].$$

Hence the modified form of Bragg's law for cubic lattice structures is :

$$\sin \theta = \frac{n \quad (h^2 + k^2 + l^2)^{\frac{1}{2}}}{2a} \qquad [4.12].$$

Since the crystal structure of Ge has atoms interspersed between the major crystallographic planes, these atoms sometimes scatter x-rays in such a manner as to prevent a maximum from occurring at the expected

Bragg angle. The planes that give reflections may be calculated from the position of the atoms in the unit cell. For the diamond lattice, which Ge is, if the following relationships occur a reflection will result.

$h^2 + k^2 + l^2 = (4n-1)$ for n = any odd integer
$h^2 + k^2 + l^2 = 4n$ for n = any even integer

The following table provides the angles for the reflections and their crystal orientation.

Reflecting plane h,k,l	Si a 5.43073 Å	Ge a 5.6575 Å	GaAs a 5.6534 Å
111	14°14'	13°39'	13°40'
220	23°40'	22°40'	22°41'
311	28°05'	26°52'	26°53'
400	34°36'	33°02'	33°03'
331	38°13'	36°26'	36°28'
422	44°02'	41°52'	41°55'

Table 4.2 X-ray diffraction angles for crystal plane.[48]

As was indicated earlier not all planes will provide a diffraction. From Table 4.2 it can be seen that a crystal oriented in the <100> will not produce a maximum interference diffraction. However since the <400> plane is coplanar to the <100> a diffraction at θ = 33°02' will occur provided that the specimen is oriented in the <100> direction.

A polished slice of single crystal Ge was placed into the X-ray diffractometer. A spectrum was recorded and is presented as Fig. 4.8. As can be seen from the data, the peak occurs at an angle 2θ = 65°57', which according to Table 4.2 corresponds to a crystal orientation in the

<400> direction.

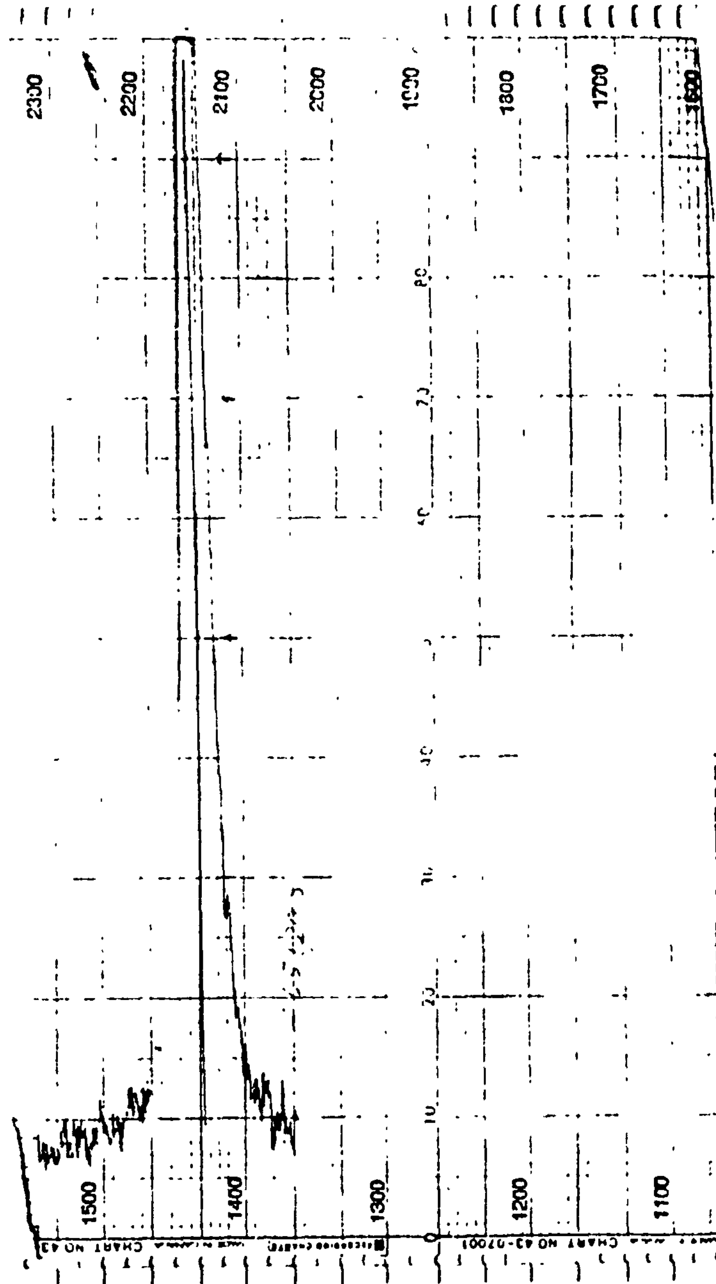

Fig. 4.8 X-ray diffraction spectrum of <100> crystal

SUMMARY AND CONCLUSIONS

An NRC vertical "Czochralski" crystal grower, built in 1962, was revitalized into working condition to perform several crystal growing operations. Originally designed to grow silicon crystals, the temperature process controls had to be retuned for the growth of a lower temperature material, namely germanium.

Upon cleaning of the grower and raw material, several attempts in growing a <111> oriented test ingot were performed. During these attempts, some successful, others not, a better understanding of the aspects involved in growing crystals were attained.

With experience and an understanding of the mechanics of heat flow at the solid-liquid interface, the successful growth of crystals became consistently easier.

A <100> oriented seed was purchased to grow several crystals with the intention of producing large area substrates for the epitaxial deposition of GaAs. The important criteria for these substrates were that they have an approximate resistivity of .1 Ω-cm as well as being n-type. The crystals had to be doped.

The doping was accomplished with a laboratory prepared doping alloy. A precise amount of this alloy was added to the charge prior to the growing process.

Following the growth of undoped and doped Ge crystals, characterization analyses were performed. Hall-Effect bulk analysis (6-point) was applied to ascertain the impurity concentration at specific locations throughout the crystal. Not only was the resistivity and impurity mobility determined but the segregation coefficient for a particular set of growing conditions as well.

REFERENCES

[1] T.J. Drummond, R. Fisher, H. Morkoc, K.Lee, M.S.. Shur, "IEEE Tr. Electr. Dev.", Vol. 30, Ed-30, p.1806, 1983.

[2] J.C.C Fan, H.K. Choi, B-Y Tsaur, G.M. Metze, G.W. Turner, "IEEE Electron Device Lett." Vol. 20, p.945 (1984).

[3] D.V. Morgan, Reliability and Degradation (Chister : John Wiley & Sons, 1981), p. 322

[4] Alan Fahrenbruch, R.H. Bube, Fundementals of Solar Cells (New York : Academic Press, 1983), p.219.

[5] H. Macksey, R.L. Adams, D. N. Mcquiddy and W.R. Wisseman, "Electron. Lett." Vol. 12, p. 2 (1976).

[6] H. Morkoc, H. Unlu, D. Zanio, C. iko, D. McIntyre, "J. Vac. Sci. Tech." Vol. 31, no. 3, p.83

[7] R.C. Bean, R. Kay, D. Zanio, C.Iko, D.McIntyre, "J. Vac. Sci. Tech." Vol. B4, p. 2153 (1986).

[8] I. Druker, Power GaAs FETS, in GaAs FET Principles and Technology, ed. by J.V. Dilorenzo and D.D. Khandelwal, (Artech House, Dedham, Massachusetts, 1982 pp 202-217.

[9] Hugh Thomas, D.V. Morgan, B. Thomas, J. E. Aubrey, G.B. Morgan, Gallium Arsenide for Devices and Integrated Circuits (London: Peter Peregrinus, 1986) p. 25.

[10] H. Unlu, H. Morkoc, "Solid State Tech. " Vol. 31, no.3, p. 71.

[11] G.C. Messenger, Milton S. Ash The Effects of Radiation on Electronic Systems (New York : Van Nostrand Reinhold, 1986), p. 445.

[12] M.G. Panish, A.Y. Cho., Molecular Beam Epitaxy, Spectrum 17(4), p.18, 1980.

[13] R. Kaplan, Surface Science, Vol. 93, p. 145 (1980).

[14] C.E.C. Woods, Progress, problems, and applications of molecular beam epitaxy, in Physics of Thin Films, ed by G. Hass and M. Francone (Academic , New York 1981).

[15] R. Fisher, et al., Electron. lett; Vol. 20, p. 945 (1984).

[16] N. Otsaka, et al., J. Vac. Sci. Tech., Vol. 84 p.896 (1986).

[17] H. Zabel, N. Lucas, R. Feidenhansl, J. Als-Nielsen, H. Morkoc Proc. Superlattices Microstructures and Devices, Aug. 17-20, Chicago (1987).

[18] A.Y. Cho, Recent Developments in Molecular Beam Epitaxy, J. Vac. Sci. tech. Vol. 16, p. 275 (1979).

[19] S.M. Sze, Physics of Semiconductor Devices (New York : Wiley, 1969) p. 850.

[20] Dash, W.C. Growth and Perfection of Crystals (New York ed by R.H. Doremus, B.W. Roberts, and David Turnbull : Wiley, 1958), p. 31.

[21] R.A. Laudise, The Growth of Single Crystals, (Prentice-Hall New Jersey, 1970) p. 191

[22] J. Czochralski, Z. Physik. Chem (leipzig) vol. 92, p. 219 (1917)

[23] G.K. Teal, J.B. Little, Phys. Rev. vol 78, p. 647 (1950)

[24] W. G. Pfann, Zone Melting (New York: Robert E. Kreiger, 1978) p.11

[25] R.A. Laudise, The Growth of Single Crystals (New Jersey : Prentice-Hall, 1970) p. 113

[26] N. B. Hannay, Semiconductors (London: Reinhold, 1959) p. 89

[27] R. Bakish, Introduction to Electron Beam Technology (New York Wiley 1962) p. 168

[28] N. B. Hannay, Semiconductors (London: Reinhold, 1959) p. 93

[29] S.M. Sze, Physics of Semiconductor Devices (New York: Wiley 1969) p. 32

[30] ANSI / ASTM F76-73 p. 353

[31] ANSI / ASTM F76-73 p. 355

[32] B.G. Streetman, Solid State Electronic Devices (New Jersey: Prentice-Hall, 1980) p. 89

[33] W. Shockley, Electrons and Holes in Semiconductors (New Jersey : D. van Nostrand, 1950) p. 78

[34] E. H. Putley, The Hall-Effect and Semiconductor Physics (New York: Dover Publications, 1968) p. 183

[35] Rolf Landauer, John Swanson, Diffusion currents in the Semiconductor Hall-Effect, Phys. Rev. Vol 91, p. 555-560 (1953)

[36] J.P. McKelvey, Diffusion Effects in Drift Mobility Measurements in Semiconductors, J. Appl. Phys., Vol 27 p. 341-344 (1956)

[37] ANSI / ASTM F76-73 p. 359

[38] ANSI / ASTM F76-73 p. 360

[39] Aldert van der Ziel, Solid State Physical Electronics (New Jersey: Prentice-Hall 1976) p.97

[40] W.G. Pfann, Zone Melting (New York: Robert E. Kreiger, 1978) p. 14

[41] N.B. Hannay, Semiconductors (London: Reinhold, 1959) p. 508

[42] W. R. Runyan, Semiconductor Measurements and Instrumentation (New York: McGraw-Hill 1975) p. 27

[43] ANSI / ASTM F389-84 p. 458

[44] ANSI / ASTM F389-84 p. 459

[45] J.I. Goldstein, Practical Scanning Electron Microscopy (New York: Plenum Press 1977) p. 3

[46] R. A. Laudise, The Growth of Single Crystals (New Jersey: Prentice-Hall 1970) p. 8

[47] W.R. Runyan, Silicon Semiconductor Technology (New York: McGraw-Hill 1965) p. 97

[48] ANSI / ASTM F26-84

APPENDIX A

If the charge weight is 500.00 grams the volume is calculated as:

$$\text{vol} = \left[\frac{1}{5.32\ \text{g/cm}^3}\right](500.00\ \text{g}) = 93.98\ \text{cm}^3$$

and if the level of doping desired is 2×10^{16} at/cm^3 then:

$$\text{total \# of atoms} = (93.98\ \text{cm}^3)(2 \times 10^{16}\ \text{at/cm}^3)$$

$$= 187.96 \times 10^{16}\ \text{at/charge of Ge.}$$

Therefore the amount of the Sb required is simply

$$\text{weight} = \left[\frac{121.8\ \text{g}}{6.022 \times 10^{23}\ \text{at}}\right](187.96 \times 10^{16}\ \text{at})$$

$$= 830.29\ \text{micrograms.}$$

APPENDIX B

If the charge weight is 710.96 grams, and the density of Ge equals 5.32 g/cm^3. Then the volume of the charge weight will be:

$$\text{Volume} = \left[\frac{1}{5.32} \right] \times 710.96 = 133.63 \text{ cm}^3.$$

If the doping alloy concentration is determined to be 5.69×10^{17} at/cm^3 and we require a resistivity of .1 Ω-cm. From Fig. 3.1 this equates to a concentration of 2.5×10^{16} at/cm^3.

∴ 2.5×10^{16} Sb (133.63 cm^3) = 3.34×10^{18} atoms of Sb/charge.

This equates to a volume of:

$$\text{vol} = \frac{3.34 \times 10^{15} \text{ at}}{5.69 \times 10^{17} \text{ at/cm}^3} = 5.87 \text{ cm}^3.$$

Therefore the mass of the doping alloy is:

$5.32 \ g/cm^3 \ (5.87 \ cm^3) = 31.235$ grams.